SOLDER JOINT RELIABILITY

A UNIFIED THERMO-MECHANICAL MODEL APPROACH

A Thesis
Submitted to the Graduate Faculty
of the
North Dakota State University
of Agriculture and Applied Science

By

Gurmukh Hiro Advani

In Partial Fulfillment of the Requirements
for the Degree of
MASTER OF SCIENCE

Major Department:
Industrial and Manufacturing Engineering

August 2014

Fargo, North Dakota

North Dakota State University
Graduate School

Title

SOLDER JOINT RELIABILITY
A UNIFIED THERMO-MECHANICAL MODEL APPROACH

By

Gurmukh Hiro Advani

The Supervisory Committee certifies that this ***disquisition*** complies with North Dakota State University's regulations and meets the accepted standards for the degree of

MASTER OF SCIENCE

SUPERVISORY COMMITTEE:

Dr. Om P. Yadav
Chair

Dr. Val Marinov

Dr. Ben Bratten

Dr. Brij Singh

Approved:

10-13-2014 — Date

Dr. Canan Bilen Green — Department Chair

ABSTRACT

Due to an unprecedented pervasiveness of electronics in high performance applications, the dependability of mission critical equipment and systems, often solely depends on the reliability of underlying embedded electronic sub-systems. This includes reliability of the solder joints which are subject to fatigue failure over time in harsh operating environments replete with thermo-mechanical stresses.

Fatigue behavior of the solder joints has been previously studied under the separate domains of microstructure evolution and non-linear plastic deformations. The proposed study captures the underlying physics of failure mechanisms to model the failure initiation and degradation phases to obtain a unified model characterizing the overall fatigue behavior over the two phases.

The model development is followed by reliability analysis which takes into account the individual phases to establish the conditional relationship for a unified reliability model. The reliability analysis has been attempted using both the failure time and the damage accumulation approaches.

ACKNOWLEDGEMENTS

I would like to extend my sincere thanks and gratitude to my advisor Dr. Om Prakash Yadav, Associate Professor, Department of Industrial and Manufacturing Engineering, NDSU, for his continuous guidance and counsel during the course of my research study. His continued close engagement and evaluation of my work helped shaped the discourse of my thesis and also with timely course correction as and when needed.

I would like to extend my sincere thanks to rest of my M.S Thesis examination committee, Dr. Valery R. Marinov (Industrial and Manufacturing Engineering), Dr. Dr. Benjamin D. Braaten (Electrical and Computer Engineering) and Dr. Brij Singh (John Deere) for constructive critical review of my thesis during the examination.

I would also like to sincerely thank Dr. Dinesh Katti, Department of Civil Engineering, Dr. Rhonda Magel, Department of Statistics, NDSU and Dr. Eunsu Lee, Upper Great Plains Transportation Institute, NDSU for their teaching, valuable academic suggestions and counselling that helped me with my academics and research.

Last but not least, I would like to extend my sincere thanks to Dawn Allmaras and other administrative staff in the Department of Industrial and Manufacturing Engineering for the support and help they rendered on administrative fronts during the course of my graduate studies at NDSU.

DEDICATION

I would like to dedicate my M.S thesis to my father Prof. Hiro Motiram Advani who was a dedicated engineer, educationist, teacher and a mentor. He exposed me to world of electrical and electronics engineering that instilled in me the intrigue and love for field of engineering. His constant encouragement for pursuit of knowledge and learning was a key factor in inspiring me to pursue higher studies alongside my career as an electronic design engineer. I would also like to acknowledge and express my deep appreciation for the support of my family in this endeavor without which this undertaking would not have been possible.

TABLE OF CONTENTS

ABSTRACT iii

ACKNOWLEDGEMENTS iv

DEDICATION v

LIST OF TABLES viii

LIST OF FIGURES ix

LIST OF ABBREVIATIONS xi

LIST OF SYMBOLS xii

1. INTRODUCTION 1

1.1. Importance of Reliability Studies 1

1.2. Research Motivation 2

1.3. Research Plan 7

1.3.1. Literature Review 7

1.3.2. Model Development 7

1.3.3. Experimental Setup and Data Collection Strategies 8

1.3.4. Data Analysis and Interpretation Strategies 8

1.3.5. Reliability Analysis 9

2. LITERATURE REVIEW 10

2.1. Solder Joint Function, Properties, Behavior and Models 11

2.1.1. Solder Joint Function 11

2.1.2. Eutectic Behavior of Solder Joints and Phase Diagrams 11

2.1.3. Mechanics of Solder Joints 15

2.2. Crack Initiation Phase in Failure of Solder Joints 21

2.2.1. Grain and Phase Coarsening 21

2.2.2. Crack Initiation and Precipitation 30

2.3. Crack Propagation Phase in Failure of Solder Joints 34

2.4. Reliability Analysis 45

3. UNIFIED MODEL DEVELOPMENT 46
3.1. Model Background 46
3.2. Model Data 47
3.3. Model Development 49
3.3.1. Crack Initiation Phase Model Development 50
3.3.2. Crack Propagation Phase Model Development 51
3.3.3. Combined Model Development 52
3.4. Unifed Model Parameter Estimation through Illustrative Example 53
3.4.1. Unified Model Parameter Calculation 54
3.4.2. Combined Model Mean Time to Fail Estimation 54
4. RELIABILITY ANALYSIS 56
4.1. Reliability Models 57
4.1.1. Failure Time Distribution Approach 58
4.1.2. Unified Reliability Model Considering Failure Time Approach 59
4.1.3. Reliability Modelling Considering Damage Accumulation Distribution Approach 60
4.2. Reliability Modelling Example 63
4.2.1. Failure Time Reliability Model Example 63
4.2.2. Damage Accumulation Reliability Model Example 64
5. SUMMARY AND CONCLUSIONS 67
BIBLIOGRAPHY 70

LIST OF TABLES

Table Page

1. Set-up and Operating Conditions for the Experiment 53

2. Estimated Model Parameters 54

3. Rate and Location Parameters for Failure Time Reliability Modelling 63

4. Location and Scale Parameters for Damage Accumulation Reliability Modelling 64

LIST OF FIGURES

Figure Page

1. Pb-Sn Alloy Phase Diagram [12] 12

2. α Phase Formation [12] 13

3. α + β Phase Formation in Eutectic Composition [12] 13

4. α and α + β Phase Formation in Near-Eutectic Composition [12] 14

5. SAC Alloy Phase Diagram [13] 14

6. Rheological Model of Solder Joint [9] 15

7. Stress Loading Profile of Solder Joint [9] 15

8. Plasticity Models [9] 17

9. Strain Rate Dependence [9] 18

10. Inelastic Response in Loading and Unloading of Material [14] 18

11. Creep Stages Under Constant Load [9] 20

12. Grain Coarsening and Fatigue Damage [2] 22

13. Average Grain Size Before and After 300 Thermal Cycles [15] 25

14. Formation of Lamellae in As-Solidified Solder Matrix in Pb-37 Solder [16] 28

15. Micro-graph Showing Shear Bands in Sn-Pb Solder [16] 28

16. Sn Depletion Due to Intermetallic Layer Formation [16] 29

17. Glide and Climb Mechanism [9] 31

18. Slip Band Movements with Solder Matrix [10] 32

19. High Stress Low Cycle Failure [10] 33

20. Low Stress High Cycle Failure [10] 33

21. Pb-Free SAC Alloy Solder Joint of BGA Package [17] 34

22. Hysteresis Loops Generated at 35°C and 150^{0}C [18] 37

23. Sn Depletion Due to Intermetallic Layer Formation [16] 38

24. Configuration Single Barrel Configuration [1] 47

25. Configuration Hour Glass Barrel Configuration [1] 48

26. Configuration Double Barrel Stacked Configuration [1] 48
27. Change in Resistance during Crack Initiation Phase 49
28. Combined Dataset for Model Parameter Estimation 53
29. Distributions of Crack Initiation and Propagation Phases 56
30. Conditionality of Degradation Phase Over Initiation Phase 60
31. Change in Resistance Distribution 61
32. Failure Time Reliability Trend 65
33. Damage Accumulation Reliability Trend 66

LIST OF ABBREVIATIONS

BGA .... Ball Grid Array

CM .... Coffin-Manson

CSP .... Chip Scale Package

CTE .... Coefficient of Thermal Expansion

CuOSP .... Copper Organic Solderability Preservative

DfR .... Design for Reliability

ED .... Electronic Design

FEA .... Finite Element Analysis

FEM .... Finite Element Modelling

PCB .... Printed Circuit Board

PDF .... Probability Density Function

PSB .... Persistent Slip Bands

RoHS .... Reduction of Hazardous Substances

SAC .... Tin-Gold-Copper

SMT .... Surface Mount Technology

TH .... Through Hole

LIST OF SYMBOLS

Ag .... Silver

Au .... Gold

Cu .... Copper

Ni .... Nickel

Pb .... Lead

Sn .... Tin

1. INTRODUCTION

This chapter is devoted to laying down the necessary background for the proposed research study titled "Solder Joint Reliability - A Unified Thermo-Mechanical Model Approach". This chapter is organized into various sections beginning with the section that lays emphasis on the need for reliability studies in the field of electronics. This is followed by the section that describes the motivation for undertaking the proposed research study. The chapter concludes with the section that outlines the proposed plan of research, steps and methodology.

1.1. Importance of Reliability Studies

Design efforts being pursued in the field of electronic design and manufacturing have seen ever increasing inclusion of requirements for reliability analysis and design for reliability (DFR). This is particularly pertinent in the view of highly demanding applications for ruggedized electronics for harsh environments such as off highway automotive (construction, mining and agricultural), on highway automotive, industrial, military and aerospace applications.

Among the factors that have a major impact on reliable performance of embedded electronic systems is the reliability of solder joints. Embedded electronic assemblies in the above mentioned applications are routinely exposed to harsh environments that include, extended exposure extreme temperature levels, slow time varying cyclical thermal stresses and large thermal loading within a very short period of time, usually referred to as thermal shocks in the industry parlance. All of the aforementioned stresses induce thermo-mechanical fatigue in the solder joints that results in crack initiation followed by degradation and eventual culmination into failure of the solder joints on the embedded electronic sub-systems. This finally results in the equipment failure leading to the equipment down time.

Needless to say, the equipment downtime results in the loss of productivity and profitability of ventures employing such equipment and eventually to decreased customer satisfaction. This in turn, results in adverse impact to the bottom line of manufacturers of these equipment's due to escalating warranty costs, decreasing sales and lost market share.

For electronic design (ED) community it has been a proposition of interest to determine an effective, data driven analytics approach to perform predictive analysis whether certain components were likely to survive given thermal shock/thermal cycling targets (in terms of number of usage cycles).

This would enable creation of a proactive approach based on reliability analysis that would enable the targeted selection of components to meet various test and field application goals. This ability would potentially result in the benefits such as, reduction or elimination of failures during test and in field (over design life time), costly tweaks and redesign iterations. Thereby, potentially garnering benefits such as reduced developmental cycle times, enhanced inherent reliability/quality within in the product, decreased over-all cost and enhanced customer satisfaction.

1.2. Research Motivation

The objective of this research study is to evaluate the solder joint reliability with an approach that encompasses a comprehensive set of degradation behaviors that lead to fatigue failure of the solder joints under various thermal stress conditions.

Exposure to thermal stresses both static and dynamic leads to induction of stresses in the solder joints and consequently set up variety of strain conditions that are precursor to eventual damage that the solder joints suffer as a result.

The solder joints under thermal stresses exhibit fairly complex phenomena due to the presence of many variables and their ensuing effects such as:

I. Material behavior of eutectic solder alloys under various thermal conditions that leads to changes in the mechanical properties of alloys at those temperature levels. Within the types of solder alloys i.e. Lead Based (Pb) and Lead Free (Pb-Free) the material constitution of alloys exhibits significant differences in the mechanical behavior under various thermal conditions [1].

II. Steady state thermal and time varying thermal stresses induce different types of fatigue behavior in the solder joints.

Therefore, an in-depth analysis of behavior of solder joints under various thermo-mechanical scenarios is foremost requirement for analyzing and predicting the reliability of the solder joints. Following sections discuss in detail the justification for the proposed study and its foundational basis.

The fatigue behavior of solder joints has been studied in great detail under the premise of plastic deformation that involves the physical phenomenon of grain boundary separation following the grain coarsening as a result of thermo-mechanical stresses. Many examples can be citied in support of this theory [2] [3] [4] which have explained this phenomenon through comprehensive constitutive modelling, experimental results and solder joint analysis. For example, in case of Pb-Sn solder, just prior to fatigue failure the grain coarsening (as a result of phase separation between Sn and Pb phases) creates grain boundaries that act as a precursor for crack precipitation. Once the crack is precipitated it sets the stage for plastic deformation through which the crack propagation and the eventual catastrophic failure follows.

The plastic region deformations are non-linear in nature and hence power law relationships like Coffin-Manson (CM) and modified Coffin-Manson models are best suited to capture the degradation behavior in the plastic regions. Coffin-Manson model proposes the stress to be proportional to n^{th} power of strain, where n is a constant depending on the material properties and environmental conditions [5]. In the area of reliability analysis though, the relevant parameter of interest is time to failure or useful life without failure. Coffin-Manson models that incorporate variable strain rates have been put forth to explain the effects of frequency on time to failure of the solder joints [5].

Most of the research based on Coffin-Manson and modified Coffin-Manson models however explains the crack propagation phenomenon very well (since it addresses only the plastic behavior and therefore the non-recoverable work phenomenon) but does not adequately explain crack initiation phase in which the significant contributor could be thermo-mechanical stresses that could over time initiate a crack [1] [2] [3] [5] [6].

The concept of crack initiation in solder joints has been very well explained using free energy phenomenon involving ability of solder joints to accommodate plastic deformation in persistent slip bands (PSBs) during stress application. This happens when movement of adjacent slip bands is stopped along opposite dislocation dipoles leading to a crack [7]. Other authors [8] have proposed models based on

Gibb's free energy change responsible for initiating the crack from state of dipole accumulation. The theory of crack initiation under Gibb's free energy model is based on the phenomenon in which a solder joint under thermo-mechanical stress is not in a state of thermal or mechanical equilibrium and causes energy to be directed towards the system. Consequently, in accordance with the established laws of thermodynamics any energy directed towards this system leads to increased entropy and therefore is not completely recovered upon removal of stresses. This irrecoverable work phenomenon eventually leads to crack initiation through grain coarsening.

On the other hand the elastic strains are predominantly linear in nature. Therefore, intuitively, it might appear that all elastic thermo-mechanical strains will lead to fully recoverable work phenomenon thereby not causing any significant degradation.

Various studies cited above have tended to concentrate on areas such as, capturing the plastic behavior phenomena, their underlying thermo-mechanical behavior, constitutive models, FEM analysis and modeling based on the experimental data. Some works have assumed the plastic phenomenon to be predominant and ignored the elastic behavior while other works have resorted to subtracting the elastic behavior in order to capture the plastic behavior [5]. The reason in neglecting the elastic stress and consequently elastic strains is based on the argument that the elastic displacements in the solder joints under thermo-mechanical stresses tend to be smaller than other inelastic displacements. Therefore, they are subtracted and total strain is argued to be solely plastic in nature [5]. This approach tends to underestimate the useful life of solder joints and the net contribution elastic deformations have on the life of the solder joints.

Works by Upadhyayula *et al* [8] have accounted for the nature of combined effects of thermal and mechanical stresses. Cyclic creep has been dealt with in the above mentioned work extensively. Creep is essentially a thermal stress induced phenomenon that is associated with the homologous temperature of the solder material. "Viscoplastic" nature of solder joint in the use condition due to high homologous temperature has been considered for analysis in above mentioned works. This suggests that the nature of deformations considered in the above study is predominantly in plastic domain.

All of the above approaches serve to understand and capture the plastic behavior of solder joint very well but do not offer much insight into the elastic behavior and therefore a significant portion of life time of solder joints that precedes this phase ends up being not considered. Inclusion of crack initiation phase in the solder joint failure modeling would provide more realistic assessment of true solder joint fatigue life and adds to the motivation for undertaking this research study.

With regards to modelling approaches, various studies have resorted to use of both the curve fitting techniques and the use of energy based models. The curve fitting approaches are referred to "phenomenological continuum models" [8]. In above study authors have argued that curve fitting models have limitations as far as extrapolation of data is concerned beyond the limits of operating conditions of the experiment that was used to derive the model. This may be partly true as far as highly non-linear regions of plastic deformation are concerned which may cause predicted values to deviate significantly if the data range used for model development is limited and does not capture the degradation behavior comprehensively. However, any data-points beyond the realms of established threshold limits for the failures should be of little interest as the failure point would be already captured in the experimental data, provided that experimental data encompasses temperature ranges that are well beyond usage range of interest.

The thought promulgated in this study is to capture the influence of thermo-mechanical stresses and strains which contribute to basic material property changes that lead to crack initiation. The motivation for the approach undertaken in this research lays in the fact that a substantial part of life of solder joints is spent enduring the stresses (without resulting instantaneous failure) that eventually precipitate the "crack initiation" followed by "crack growth" to the point of eventual failure [1]. This very fact points to "inherent resilience or strength" present in the solder joint from the time it is formed and thereafter it is acted on by combination of thermo-mechanical stresses namely, elastic, creep and plastic. Elastic behavior intuitively should be predominant during initial life of solder joint before the joint undergoes material property changes and becomes a plastic system where upon irreversible deformation begins to take place.

A few studies [9] have pointed out that under low strain rate scenarios of thermo-mechanical loading, the fatigue life in the crack initiation phase is relatively short which according to some studies could be only 10% of total life. However, low strain rate cycles are associated predominantly with creep behavior and therefore should account for viscoplastic phenomenon. In his paper, Wild [10] has proposed that under cyclic loading the life of solder joint is enhanced due to the compressive forces at play which often impart strength to the solder joint. This is consistent with solder joint reliability study for both the Pb-Sn and Pb-free solders that shows the crack initiation phase to be about 50% of total life [1].

Some authors [11] have addressed the issue of initiation time before degradation in order to estimate the degradation free time in products. They have pointed out that this approach can be beneficial in many efforts directed towards improving the product reliability by concentrating on factors that can help prolong either the initiation phase or the degradation phase.

Irrespective of the amount of time spent in the crack initiation phase, the undertaken research can not only offer valuable insight into degradation phenomenon but can help pave ways towards designing optimization strategies to prolong the crack initiation phase. Understanding underlying behavior in a comprehensive manner can go a long way in optimizing the design parameters to mitigate the effects of factors that play a role in the grain coarsening phase. This in turn can help in establishing DFR criteria for solder treatments, recipes, processes, PCB design and component selection. It also provides more realistic reliability assessment by capturing both the initiation and the degradation behavior under the influence of thermo-mechanical stresses.

Therefore, not accounting for initiation time, into the fatigue failure time analysis doesn't do justice to holistic approach to the reliability studies involving solder joints as it tends to underestimate the useful life predictions. Furthermore, the variability in material properties, manufacturing processes, operating conditions and other factors like the variety of components comprising a given electronic assembly, pad geometries, PCB variations etc. also influence the fatigue behavior of the solder joints. This study also considers the probabilistic behavior of the fatigue phenomena of solder joints and therefore provides a better reliability analysis to predict the solder joint behavior.

1.3. Research Plan

This section describes the broad plan and methodologies that are proposed to be adopted to purse the various stages of the research being undertaken. The steps entailed in the entire process are mentioned below under individual headings.

1.3.1. Literature Review

A comprehensive literature review is proposed to be carried out to establish the grounds for proposed research titled - *A Unified Thermo-Mechanical Model for Solder Joint Failure and Reliability Analysis*. The literature covering the research and work carried out in this field thus far, will be dealt with to establish the motivation for this research study. This is proposed to be addressed with regards to approaches taken so far that have tended to deal with solder joint failure under two separate domains of micro-structure evolution and plastic domain degradation. Also proposed is additional comprehensive literature review to gather the foundational basis of the constitutive work-energy related degradation models for solder joints. Additionally, literature review is proposed to be performed on publications that have dealt with approaches similar to proposed research and build on the knowledgebase already established.

Therefore, overall endeavor of this phase proposes to establish the foundational theory, and identify quantifiable and measurable physical attributes or quality characteristics that are a direct result of grain coarsening and degradation phenomena to develop an integrated model that mathematically defines the selected parameter as a function of thermo-mechanical stresses with respect to time.

1.3.2. Model Development

The constitutive model development is proposed to be undertaken entails starting with the basic mathematical models established through earlier research and use those to develop mathematical relationships that represents the defined quality characteristic or measurable parameter of interest i.e. the resistance of solder joint as a function of time and thermo-mechanical stresses.

The resistance of a solder joint is easily measurable quantity that is dependent on the way volume is physically distributed. Therefore, a constitutive model that equates the change in resistance

over time to energy relation that incorporates temperature as another measurable parameter would provide both constitutive model and the necessary framework experimental set-up. Thus, the underlying grain coarsening and degradation phenomenon can be interpreted in terms of change in resistance. Due to inherent nature of fault the crack precipitation should result in abrupt change in resistance from a previous constant value. In order to account for normal tolerances and measurement errors a sustained / permanent fixed percentage increase over previous level will be proposed to establish the thresholds for crack initiation and failure time.

1.3.3. Experimental Setup and Data Collection Strategies

Having adequately defined the constitutive model strategy above, defining the experimental setup and data collection strategy becomes the next step.

The experimentally collected dataset is proposed to be used for the study. A given set of solder joint entities comprising standard surface mount technology (SMT) packages soldered on the PCB using standard reflow processes, is proposed to be used. This set-up is proposed to be subjected to thermal stresses in a calibrated environmental test chamber and wired for precision time stamped resistances measurements.

Thus, all the time stamped state parameters of interest (temperature and error voltage and therefore resistance) are proposed to be collected for purpose of data analysis. The test is proposed to be run till point of catastrophic failure.

1.3.4. Data Analysis and Interpretation Strategies

The time stamped parameters/quality characteristics are proposed to be used in constitutive model equations to interpret the length of time it takes for crack initiation and for degradation process to result in a failure. The collected data will be used to for estimating the model parameters for combined crack initiation and degradation phases.

1.3.5. Reliability Analysis

The model discussed in section above is only able to predict the mean life times for various phases and the failure time. In order to evaluate the reliability of solder joints the distribution parameters will be evaluated to determine the failure time and the damage accumulation reliability. Total reliability for two models will be evaluated and compared.

2. LITERATURE REVIEW

This chapter focuses on the literature review with the objective of presenting an overview of the papers and other publications by various authors, online articles and textbooks that have been studied and referred to pertaining to the area of undertaken research. First part of the undertaken research seeks to develop the unified model that is able to predict the time to failure for solder joints under study based on given set of experimental data and operating conditions. Second part of this study deals with the reliability modelling and analysis using failure time and damage accumulation approaches. Given the aforementioned plan the literature review presented in this chapter is organized to ensure alignment with underlying thought and overall fame-work of undertaken research. This includes both the crack initiation and the crack propagation phenomena for a unified solder joint modelling and reliability analysis. The literature review presented below is therefore organized and presented under following broad areas:

I. Solder Joint Behavior, Properties and Modelling: This area covers researching literature concerning background theory regarding behavior and properties of eutectic solders joints and constitutive thermo-mechanical stress strain models.

II. Crack Initiation Phase in Solder Joints: This area covers phenomenon of grain growth, nucleation and voiding and surface energy reduction under thermo-mechanical stresses leading to crack formation/initiation.

III. Crack Propagation Phase in Solder Joints: This area covers phenomenon of stress relaxation, grain boundary sliding and stress flow and ensuing plastic deformations resulting in degradation and eventual failure of solder joint under the influence of various thermo-mechanical stresses like creep and plastic degradation as described predominantly through Coffin Manson and Modified Coffin Manson models.

IV. Reliability Modelling and Analysis: This area covers reliability models that deal with the situations of combined initiation and degradation phenomena.

2.1. Solder Joint Function, Properties, Behavior and Models

This section deals with the foundational aspects and theory relating to function, material properties and behavior of solder joints. These foundational aspects are a key to building comprehensive understanding of solder joints in operating environments and exposure to thermo-mechanical stress.

2.1.1. Solder Joint Function

Basic function of solder joint is to provide a strong electrical and mechanical bond between electronic components and the PCB, thereby providing a mechanically robust and low impedance electrical interconnection between various components that comprise circuit(s)/sub-circuit(s). While on one hand evolution of electronics has led to proliferation of huge variety of components, on the other hand however, Pb-based or Pb-Free eutectic solders continue to be the mechanism of choice for bonding components to PCBs.

Apart from relative easy availability of constituent raw material comprising solder alloys, well-established soldering processes using Infra-Red Reflow, Wave and Selective Solder machines allow for very high quality, high precision manufacturing of electronic assemblies in large quantities at low cost and reasonably fast pace. Moreover, metallic solder medium offers various other advantages in terms of desirable metallurgical properties like favorable thermal properties and relative stability over wide temperature ranges that are essential pre-requisites for reliable performance of electronic circuits.

Other bonding techniques involving conductive resins etc. not only, do not offer same degree of advantages, they also present challenges like long curing and treatment times aside from storage, handling and other process complexities.

Therefore, soldering process has been and shall continue, in the foreseeable future, to be the mechanism of choice for bonding the components to the PCB.

2.1.2. Eutectic Behavior of Solder Joints and Phase Diagrams

In order to build a sound and comprehensive model that explains the solder joint degradation over time, it is imperative to explore the pathways that lead to genesis of the problem followed by its proliferation.

Figure 1 below represents the phase diagram for Pb-Sn alloy. It shows various phases of the constituents of alloy with regards to temperature and their percentage weight ratio in the alloy.

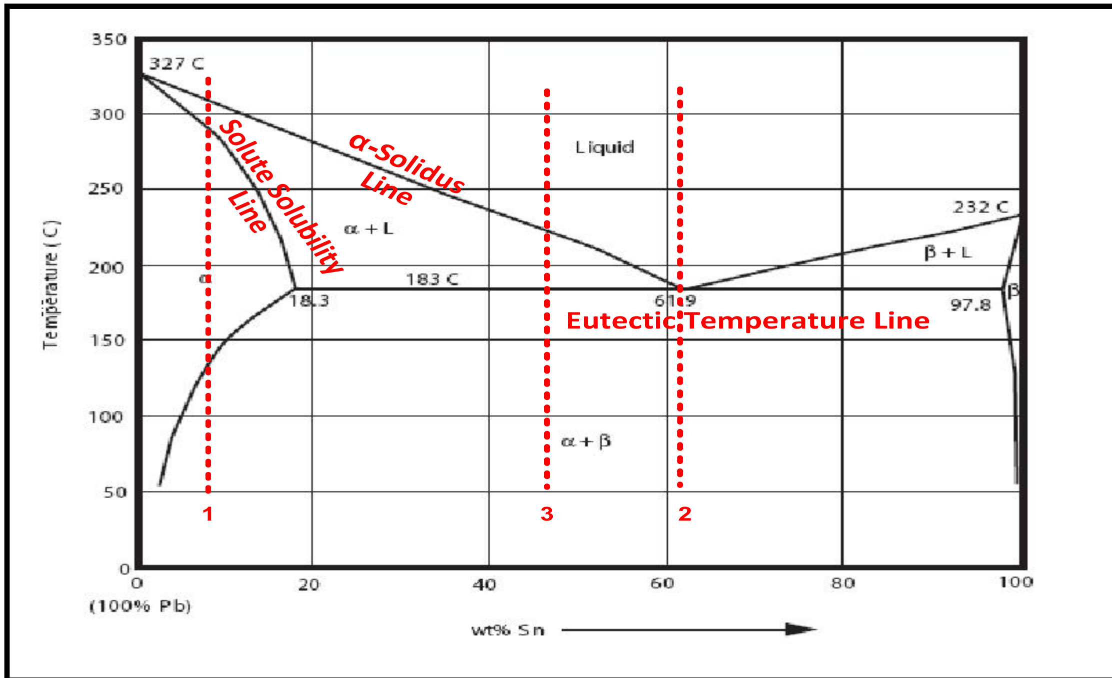

Figure 1. Pb-Sn Alloy Phase Diagram [12]

Behavior of the Pb-Sn alloy can be explained with help of 3 states as shown by dotted lines marked 1, 2 and 3. Though the figure above represents the behavior of Pb-Sn alloys the phenomenon of nearly single phase alloys such as Pb-free SAC alloys can also be very well understood from the behavior of Pb-Sn alloys shown in the Figure 1 above and as explained below:

I. In case of line 1 the alloy predominantly consists of α phase. Therefore, as the temperature drops the alloy transitions from liquid to solid phase as shown in Figure 2.

II. In case of line 2 the alloy composition will be a eutectic alloy which passes through eutectic point as it solidifies. As the temperature drops the alloy transitions from liquid to solid phase as shown in

III. Figure 3.

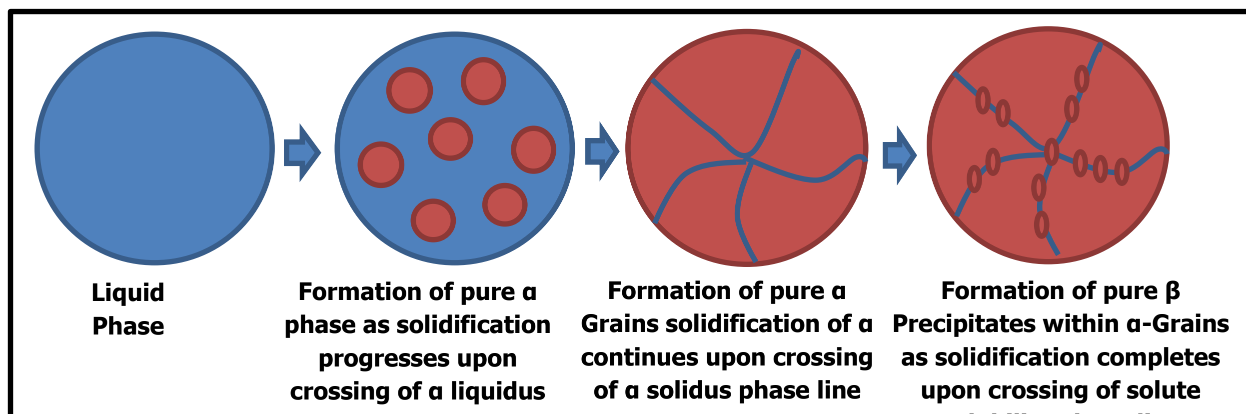

Figure 2. α Phase Formation [12]

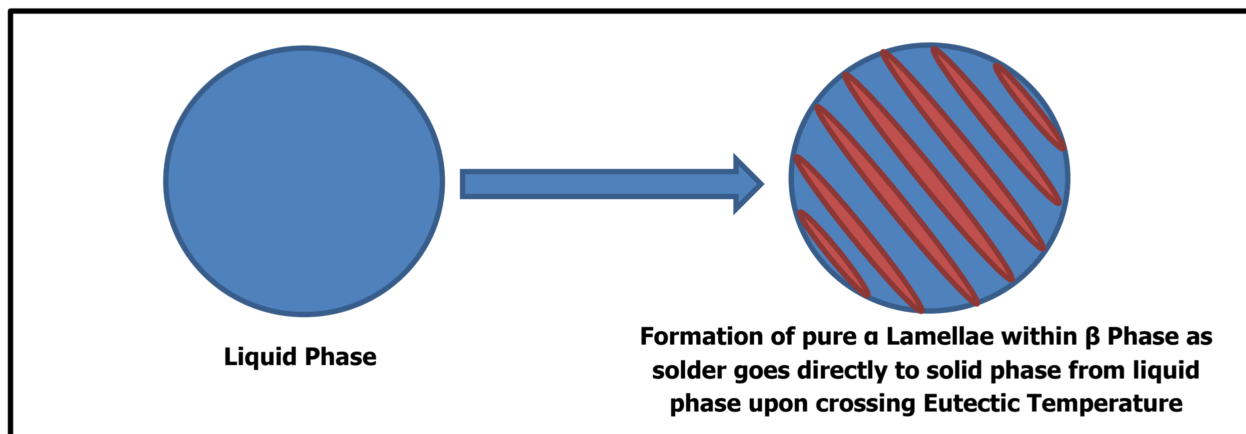

Figure 3. α + β Phase Formation in Eutectic Composition [12]

IV. In case of line 3 the alloy composition is near eutectic in which one component (Sn in this case) is in liquid phase all the way up to eutectic temperature. Whereas, volume composition of other component (Pb) keeps on increasing as the temperature drops and solidification progresses. However, since the composition of this alloy is not dominated by Pb alone, hence, not all Pb will precipitate at once with the Sn. Upon reaching the eutectic temperature remaining Pb along with Sn will solidify in form of Lamellae in a structure on dotted by Grains formed due to earlier precipitation of Pb as represented in the Figure 4 below.

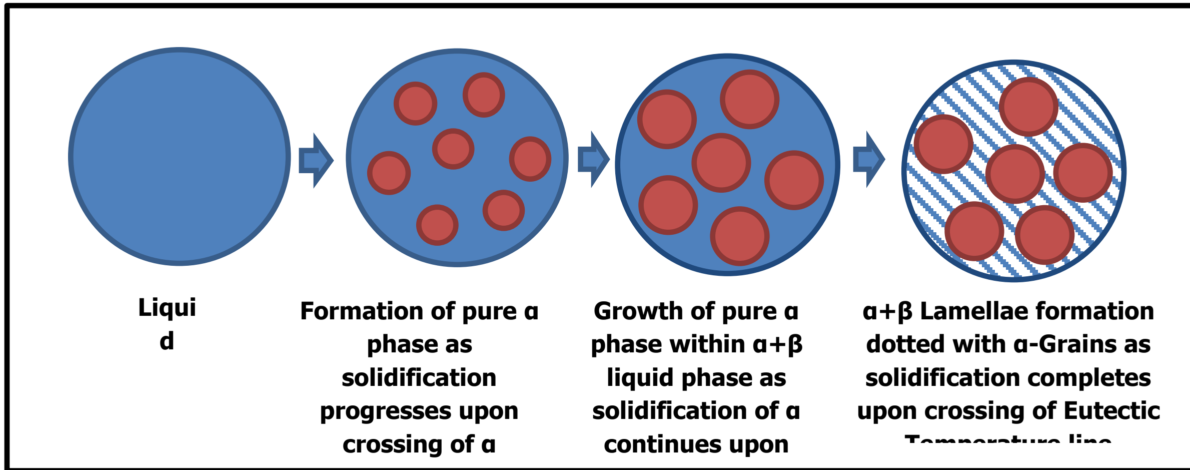

Figure 4. α and α + β Phase Formation in Near-Eutectic Composition [12]

Figure 5 below represents the phase diagram of Pb-Free SAC alloys. These alloys are dominated in weight concentration by a single component, which, in this case is Sn. Behavior and composition of these alloys is best explained by bullet point IV above for Pb-Sn alloys.

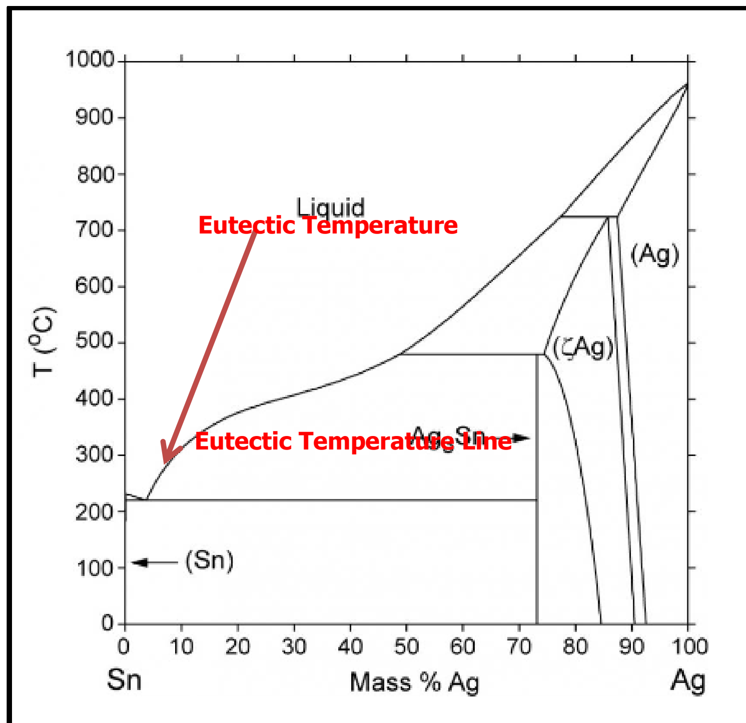

Figure 5. SAC Alloy Phase Diagram [13]

2.1.3. Mechanics of Solder Joints

The basic underlying theory and physics of solder joint failure mechanism, though a very complex phenomenon, can be adequately explained through the comprehensive treatment of material science of the solder joint and mechanical stress-strain theory under the influence of thermal stresses. The thermal stresses result induction of mechanical stresses in the solder joints due to relative motion between the electronic component(s) and the PCB owing to difference in coefficients of thermal expansion (CTE) of the PCB and the components. The "Rheological Model" that represents the practical solder joint behavior is shown in Figure 6 below:

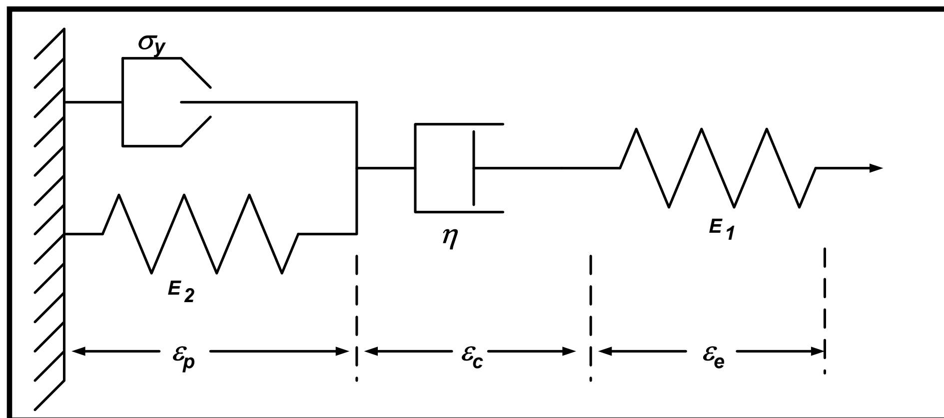

Figure 6. Rheological Model of Solder Joint [9]

When subjected to real world application the solder joints are subjected to thermo-mechanical stresses which generate the loading profile shown in Figure 7 below.

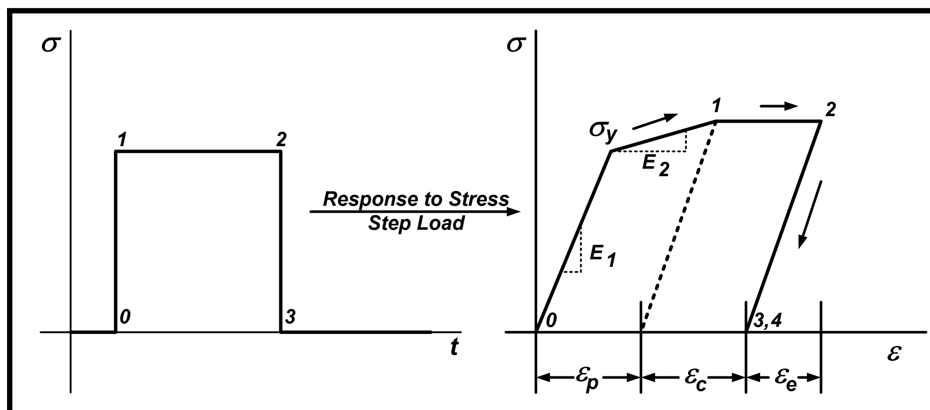

Figure 7. Stress Loading Profile of Solder Joint [9]

The total strain in the solder joint is given by following equation:

$$\varepsilon_{tot} = \varepsilon_p + \varepsilon_c + \varepsilon_e \qquad (1)$$

where, the symbol ε represents strain and subscripts p, c and e represent plastic, creep and elastic strains respectively. Relative mismatch between the CTEs of various components bonded by the solder joint results in relative motion which gives rise to strain phenomena that primarily comprises following 3 types:

2.1.3.1. Elastic Strain

The element represented by spring E1 exhibits elastic strain characteristic of the solder joint. This means that each time the stress is applied, it will expand by an amount proportional to applied stress. Upon withdrawal of applied stress will contract back to its original shape without suffering permanent deformation. It follows Hooke's Law which is given as:

$$\varepsilon_p = \sigma / E \qquad (2)$$

where, σ is the stress applied in MPa and E is the Young's Modulus of elasticity in MPa.

2.1.3.2. Plastic Strain

Plastic strain is time dependent non recoverable deformation as a result of non-recoverable work due to inelastic strains. As the material is loaded up with stress it induces strain. At a critical stress level σ_y permanent deformation begins to occur. Figure 8 below shows three plastic domain stress-strain scenarios that can occur.

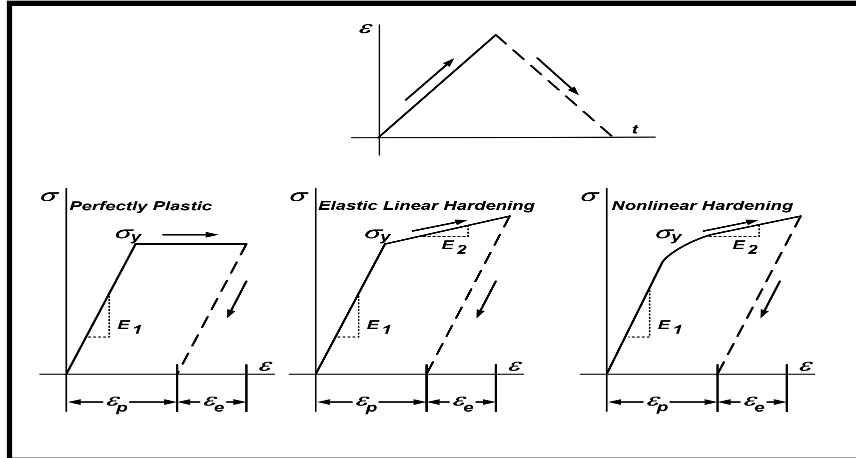

Figure 8. Plasticity Models [9]

The three scenarios depicted in Figure 8 are:

I. Perfectly Plastic Deformation: In this case the deformation will have no hysteresis loop whatsoever and no elastic return path return path due to which the material will deform completely.

II. Elastic Linear Hardening – the plastic deformation follows a deviation from initial linear path to another linear path with different slope. This is indicative of the fact that when the stress is removed the material will not completely regain its original form factor and hence the return path will follow a hysteresis loop

III. Non Linear hardening – the plastic deformation follows a nonlinear path and characterized by Ramsgood-Osgood equation given below:

$$\sigma = H(\varepsilon_p)^n \tag{3}$$

where, H is a material constant set to a stress value when $\varepsilon_p = 1$ and n is material constant called strain hardening exponent.

Close observation of equation (3) reveals power law relationship and its similarity to Coffin-Manson models. Even though theoretically plastic strain is a time independent phenomenon but studies [9] have shown that this property is very much dependent on "strain rate". The said studies have shown that for plastic strain to exhibit time independence the strain rate has to be 2%/sec or more. Lower strain rates exhibit creep again may be due to larger dwell time associated with very low strain rates as they

would indicate that stress levels are more or less constant (again alluding to higher dwell time). This is shown in the Figure 9 below.

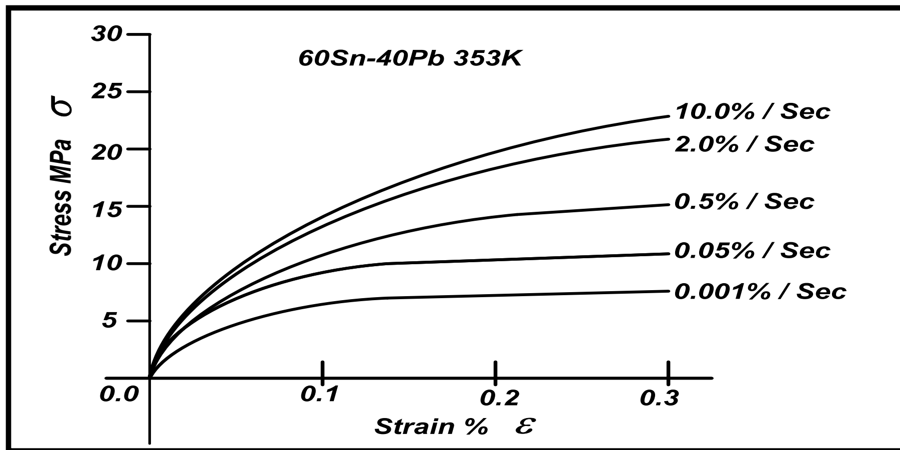

Figure 9. Strain Rate Dependence [9]

2.1.3.3. Material Behavior during Tension and Compression

The tension/compression tests with low strain rated on annealed metallic specimen yield following is shown in Figure 10 below:

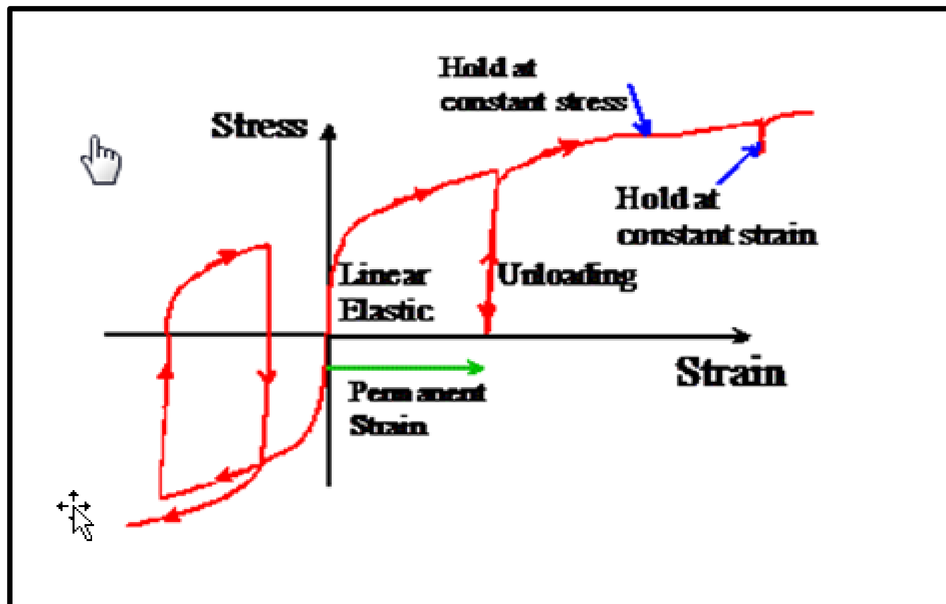

Figure 10. Inelastic Response in Loading and Unloading of Material [14]

Sequence of Stress Strain relationship shown above results in following observations:

I. For modest stresses and strains the solids respond elastically. Stress = k*Strain

II. If Stress > $Stress_{critical}$, then Stress = $k*Strain^n$ and the stress strain curve will curve gradually leading to permanent change in dimensions of specimen upon unloading.

III. If Stress is removed during the test the stress strain curve during unloading has slope equal to elastic part of stress strain curve. If the specimen reloaded it will retrace the last curve until stress again reaches the maximum value during prior loading and which point it will leave linear path and become non-linear. At this point permanent plastic deformations again begin to set in.

IV. If the specimen is now held at constant strain, which means that the applied stress is reduced or relaxed, in order to maintain same strain (as the system is now in plastic region) and unloaded and loaded again the system will behave as if it was elastically unloaded. Similarly if the system is loaded with constant stress it will generally deform plastically at a very small rate. This phenomenon is called creep.

V. For small strains the mirror reversal of stress strain relationship is true.

VI. If the specimen is subjected to compression first and tension later it will enter plastic deformation at lower stress than it would normally if it was subjected to tension first. This is known as Bauschinger Effect.

VII. In event of cyclical loading the materials may harden or soften.

2.1.3.4. Creep Strain

Creep strain is most easily demonstrated by holding material under constant stress for long periods of time and observing ensuing deformation increasing over time. Damper η in figure 1 represents creep. There are 3 observable phases of creep shown in Figure 11 below:

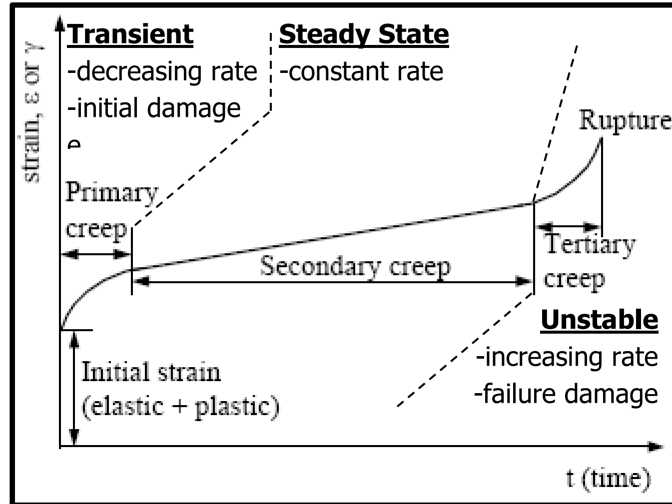

Figure 11. Creep Stages Under Constant Load [9]

The initial portion of the first phase called the Transient Phase as shown in figure above is consistent is with proportional stress strain relationship. This is followed by non-linear phase where the strain rate seems to decrease with respect to time. This is the stage where the solder matrix undergoes stress relaxation and hence the proportional relationship between the stress and strain is lost.

Second stage as shown in the Figure 11 above is called Steady State Phase. In this phase the flow stress required to maintain the plastic deformation of the solder matrix is more or less constant. Therefore, we see a constant strain rate with respect to time.

This is followed by the third stage labeled as Unstable in Figure 11 above. This is the stage where strain rate required maintain is no longer constant and the solder begins to experience the damage due to creep.

Other details regarding characteristics of creep strains, constitutive models and its role in crack initiation are discussed in section 2.2.2 below:

2.2. Crack Initiation Phase in Failure of Solder Joints

Solder is a high surface energy material and is therefore, inherently unstable. Upon being subjected to thermal stresses and aided by mechanical stresses or a combination thereof, the material absorbs the incoming energy directed towards the solder joint system and returns to equilibrium state of low surface energy. This process takes place through gradual phase and grain coarsening that weakens the solder joint structure due to reduction in net surface area of contact, consequently, making it susceptible to failure in areas of high stress concentration.

2.2.1. Grain and Phase Coarsening

It is a well-established fact that one of the main precursors to fatigue fractures in materials undergoing thermal, mechanical and thermo-mechanical stresses is change in grain structure of the material. The initial degradation of solder joints itself manifests the changes that involve coarsening or nucleation of the grains leading to reduction on surface energy and in the process giving rise to the voids within the material structure.

This problem is further compounded when the system under stress is inherently non-homogenous such as the solder joint [2]. The non-homogeneity comes into effect due to dissimilarities between the surfaces bonded together by the solder material such as:

I. Component Lead/Terminal Finish: Component terminals these days (due to increased RoHS compliance) are mostly Sn plated and in some cases for special requirements can be Au (Gold) plated. The function of outer plating is to impart a stable surface finish and good wetting properties (high surface energy finish) to terminal contacts that are usually constructed of more sturdy materials such Cu (Copper) and Ni (Nickel). While Cu has good wetting properties but it is fairly unstable when exposed to air hence it needs to be plated with more stable finish. Ni on other hand does not have good wetting properties being low surface energy material hence it needs to be plated with material that has good wetting properties.

   The materials of choice for purpose of plating the terminals are either Sn or Au. Thus this process creates high surface energy layer which reacts with the molten solder to create

intermetallic layer. In case of both Pb-Sn and Pb-Free solders, soldering process temperatures cause the Sn and Au plating on the component leads to melt and react with Sn from solder to form intermetallic compounds with Au and Cu. This process leaves Pb-rich phases in case of Pb-Sn solders and a layer of Sn/Cu, Sn/Au and Sn/Cu/Au intermetallic grains ready to undergo growth and coarsening when subjected to thermo-mechanical stresses.

II. PCB Pad Finish: Similar to the case of component lead finishes explained above, PCB component pads are also plated to impart them with stable finish with good wetting properties. These in turn cause grain coarsening due to depletion of Sn Phase in case of Pb-Sn Solders and due to formation of Sn based intermetallic with the PCB pad metals which are mainly Au, Ag(Silver), CuOSP over Cu Pads and Sn-Pb. Formation of intermetallic leaves the coarsened grain structure as is also shown in Figure 21.

As stated earlier the solder material is inherently a high surface energy material and is therefore inherently unstable. Upon being subjected to thermal stress and aided by mechanical stresses or a combination thereof, the material in solder joints absorb the incoming energy directed towards the solder joint system and return to equilibrium of low surface energy state.

This process comes at cost of degradation of the solder joint structure which leads to grain growth or nucleation that results in surface area reduction and eventually leads of voiding within the solder joint matrix. The sequence portraying the degradation phenomenon is shown in the Figure 12 below:

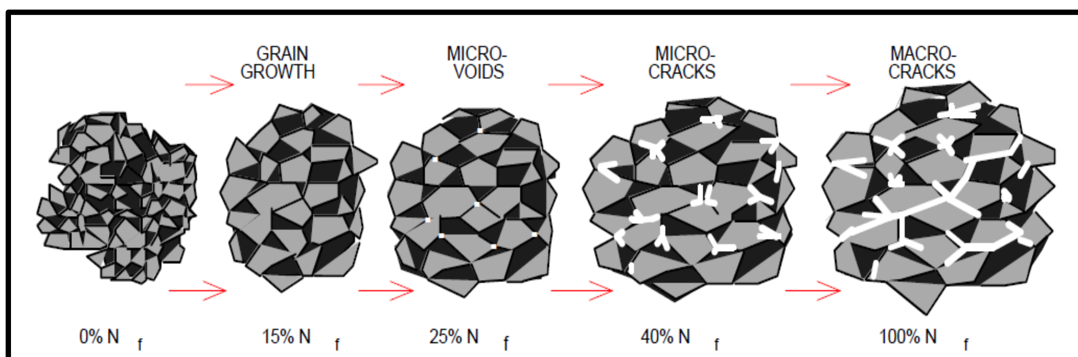

Figure 12. Grain Coarsening and Fatigue Damage [2]

Further insight into this phenomenon is given in [3]. According to this paper the grain boundaries are areas of high potential energy and hence the primary driving force in single phase materials. As the grains grow by combining into larger particles the total interfacial energy gets lowered.

In multiphase systems the thermodynamic basis for phase coarsening is combination of driving force mentioned above and Thomson-Freundlich solubility relationship [3]. According this theory, the solute concentration in the matrix (adjacent to the particle) increases with the decrease in the radius of curvature of interface. This leads to formation of concentration gradient in the matrix causing the solute to diffuse in the direction of largest particles. As the process of diffusion goes on, it causes smaller solute particles to dissolve raising the concentration and this result into more particles diffusing towards the large particles leading to coarsening. In theory this process continues until the system is phase separated.

From mathematical perspective, one of relations that gives the rate if change of area of individual grain cell is given below:

$$\frac{dA}{dt} = \frac{1}{3}.\pi.\sigma.k.(n-6) \tag{4}$$

where, k is diffusion constant, σ is specific grain boundary energy and n is number of sides in a cell.

Another model for diffusion controlled coarsening is given as:

$$r_f^3 - r_0^3 = D.\gamma.x_e.t \tag{5}$$

where, D is diffusion coefficient, γ is interfacial energy, x_e is equilibrium solubility, t is time and $r_f^3 - r_0^3$ represents change in volume.

Modeling technique has been proposed [8] for fatigue damage initiation due to plastic cyclic plasticity and cyclic creep. These studies involved Pb-Sn solders and they have provided conceptual foundation to quantify fatigue damage due to thermo-mechanical stresses.

Authors state that many empirical relations that exist to explain the fatigue behavior of solder joints cannot be used for accurately extrapolating the behavior beyond the ranges over which they were established. This however can be countered with an argument that this situation may never arise if the

stress levels initially considered to derive the model were comprehensive enough and covered the ranges beyond what can be expected in operation.

Another justification for using micro-mechanical approach given by the authors is that during the reliability testing and other qualification testing, the micro-structural evolution of solder joint under accelerated conditions might be quite different from that in real life operation. Hence, empirically determined models derived using test profiles may not be applicable to in operation conditions.

Of particular interest with regards to subject of present research is the micro-structural coarsening and its implications not only on the grain coarsening and grain size under the influence of thermo-mechanical stresses but also its effects on other measurable parameters and properties such as the solder joint resistance.

Micro-Structural coarsening increases with increasing strain rates in two-phase alloys such as Pb-Sn solders. As has been stated before in the review sections above, these strains come into play due to CTE mismatches among various entities of solder joint system. Widely accepted model that explains the coarsening phenomenon is "Cubic Coarsening Model" given as:

$$d^3(t) - {d_0}^3(t) = \frac{c_1 . t}{T} \exp^{(-\frac{\Delta H_g}{RT})} \quad (6)$$

where $d^3(t)$ is mean phase diameter at time t, ${d_0}^3(t)$ is phase diameter at time t=0 (as solidified), c_1 is kinetic factor in μm^3-K /h, ΔH_g is activation energy, R is gas constant and T is absolute temperature.

Above relation (6) does not incorporate effect of mechanical strains due to thermo-mechanical stresses and therefore authors propose modified generalized expression given below:

$$d^3(t) - {d_0}^3(t) = \frac{c_1 . t}{T} \exp^{(-\frac{\Delta H_g}{RT})} \left[1 + \left(\frac{\Delta T}{c_2}\right)^{n_c}\right] \quad (7)$$

Above expression reinforces the underlying idea that grain coarsening will occur until equilibrium is reached (first order saturation) and will not continue indefinitely.

Equation (7) also forms the fundamental basis of underlying parametric manifestation of another material property i.e. the resistance of solder joint that can be utilized to study and model the fatigue behavior.

Pb-Sn solder is "rate sensitive" heterogeneous system that has high homologous temperature due to low melting point and good wetting properties. This suggests that in liquid phase it has high surface energy [15]. Since thermo-mechanical events cause grain coarsening hence progression to heterogeneous phases should happen due to rate of change of these thermo-mechanical events which lead to reduction in surface energy due to grain growth.

At typical cooling rates during manufacturing process of electronic assemblies, isolated and successive Pb islands are formed within Sn matrix. At cast Pb-Sn alloy has very high surface per area per unit volume and is therefore thermodynamically a very unstable material.

Exposure to thermo-mechanical strains causes evolution of coarser equiaxed grain structure leading to minimization of surface energy. This is followed by grain boundary sliding, grain rotation, void growth and coarsening. Just the thermal events alone can induce grain coarsening and mechanical strains (CTE mismatches) then lead to further grain growth.

Strain might lead to movement of PSBs causing like Pb Structure to come into contact with each other leading to Pb crystal growth. As the Pb crystals grow they lead to overall reduction in the surface area of Pb with Sn and reduction in the energy of Pb-Sn System. All these phenomena are time dependent. The phenomenon above is captured in the Figure 13 below which shows solder cross section before and after thermal cycling.

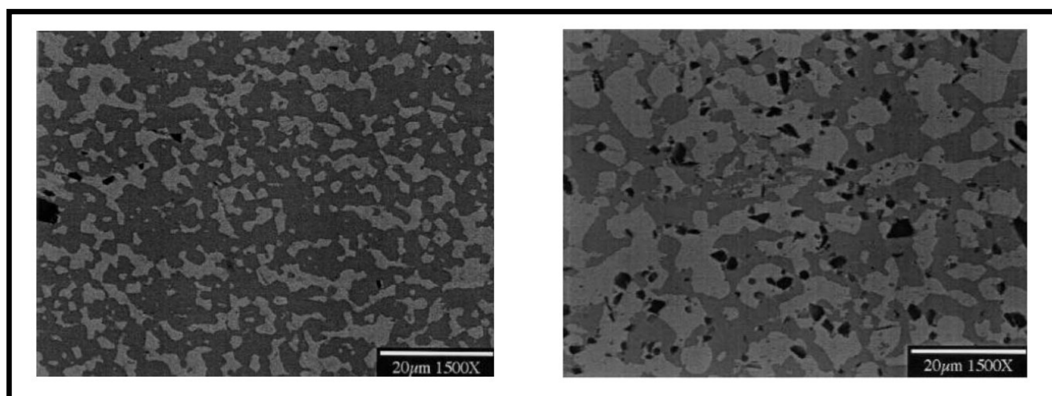

Figure 13. Average Grain Size Before and After 300 Thermal Cycles [15]

The micro structure of evolution of solder during manufacturing depends on the interactions of solder with the metals on component terminals and PCB substrates to form intermetallic layer and their

solidification rates [16]. Later on in in service depends on the influence of thermo-mechanical stresses. All these above mentioned factors lead to formation of different grain structure and variability in life.

Most solder joint failures occur at the interface of the components and solder matrix and can be categorized into 3 broad categories:

I. Tensile Strength Failure: Due handling or drop as a result of exceeding ultimate tensile strength.
II. Thermal Fatigue Failure: Due to fatigue in service mostly due to cyclical thermo-mechanical stresses.
III. Dimensional Changes: Due to stress induction and stress relaxation.

Authors point out that even though the chemical composition of solder is well known, the lack of knowledge regarding microstructure evolution makes the task of solder joint reliability becomes difficult. This is clearly pointed out in the fact that while the chemical composition of solders can be same there can be huge variation in the fatigue life due to the variability in factors that govern micro-structure evolution of solder.

According to authors neglect of solder micro structure evolution has not caused wide spread problems primarily because in electronic manufacturing the tight process control ensures uniform and fast solidification rates that result in the micro-structure that does not exhibit much variability overall. This leads to similar behavior in the field as well. Moreover the experience gets empirically codified and gets transferred to other products and designs.

Authors also dwell on the difference in performance of lab specimens and the manufactured assemblies. One such difference exists between the bulk studies in lab involving test specimens (1) and manufactured electronic PCB assemblies. Primary difference in the two scenarios is two-fold. Firstly, the test specimen and components have different surface finishes and therefore chemistry of intermetallic is different due to formation of different types of intermetallic compounds primary grain formation. Secondly, the bulk lab specimens cool at much slower rate compared to manufactured assemblies and hence they result in different micro-structures as compared to manufactured assemblies. Studies have pointed out slower cooling rates contribute to a micro-structure that causes significantly lower strains to

failure and shortened fatigue life of lab specimens compared to manufactured assemblies that undergo rapid cooling rates.

Two areas of paramount importance from this paper with regards solder joint reliability are:

I. Micro-structure evolution as after the soldering process.

II. Micro-structure evolution during service.

Intent of solder is to also "wet" the surfaces to be soldered hence it is by nature "high surface energy" compound. During soldering process the molten solder undergoes reactions with surface metals on the substrates to form intermetallic compounds. In most cases the Sn combines with Cu, Ag or Au to form the intermetallic compounds leaving behind the matrix rich with other component of initial eutectic solution. In case of Pb-Sn solder the solder matrix just beyond the intermetallic is Pb rich. This Sn depleted matrix is a perfect environment for Pb to recrystallize into larger grains under the influence thermo-mechanical stresses. The most common intermetallic compounds are Cu_3Sn and Cu_6Sn5.

During service as-solidified material starts out as out of equilibrium and is often used in high homologous temperature environment. Authors point to 3 out of equilibrium conditions.

Firstly, the as solidified eutectic material is out of equilibrium in composition and volume fractions. As the eutectic solution solidifies it solidifies into mixture of terminal solid solutions as per the compositions given by terminal points of eutectic line. As the temperature is lowered the solute content in the solution decreases (due to solute phase solidification). Since solid state diffusion is low hence baring few fine precipitates Sn in Pb, the Pb and Sn phases arrange themselves in lamellae as shown in the Figure 14.

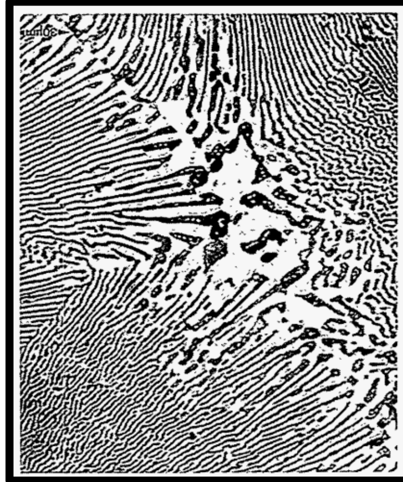

Figure 14. Formation of Lamellae in As-Solidified Solder Matrix in Pb-37 Solder [16]

Secondly, as solidified eutectic solder is out of equilibrium with respect to changes that decrease area per unit volume. This is evident due to good wetting properties of solder and the formation Lamellae in the solidified solder. The process of transitioning to low surface energy occurs through the gradual *recrystallization and spheroidization* of lamellae due to temperature related diffusion and due to spontaneous recrystallization due to mechanical deformations. The recrystallization occurs along the bands of in homogenous shear as shown in Figure 15 below.

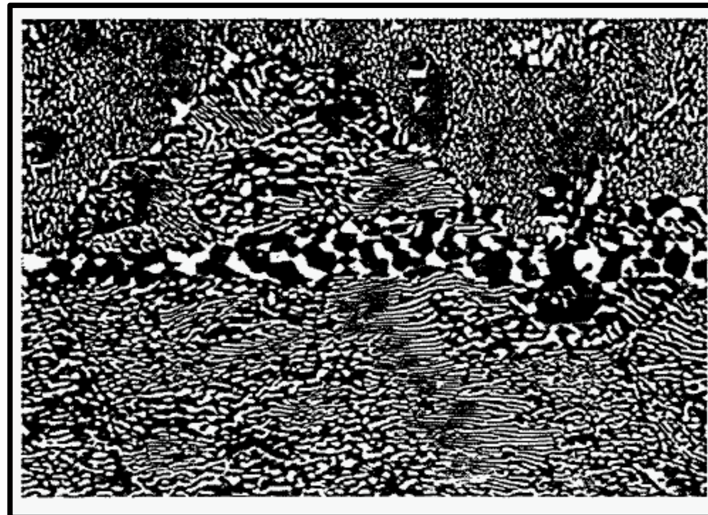

Figure 15. Micro-graph Showing Shear Bands in Sn-Pb Solder [16]

Thirdly, as solidified eutectic solder is out of equilibrium with respect to gradual growth of reactant phases. This is so because the formation of intermetallic layers causes depletion of Sn from the

material adjacent to substrate solder interface. This problem is more compounded in Pb-Sn solders as compared to Pb-free. This is shown in Figure 16 below.

Figure 16. Sn Depletion Due to Intermetallic Layer Formation [16]

Having addressed the issue of micro-structure evolution the authors have proposed the degradation models under the influence of creep, stress relaxation and creep fatigue. Understanding of all these three phenomena is important for present undertaking in developing the comprehensive model that explains solder joint behavior.

Various environmental conditions and their effects on creep behavior of solder material have been dealt with in [17] . Vibration and mechanical shock can be a problem for die-level interconnects such as die connected to heat sink. Though it is not mentioned in the publication [17], Pb-free alloys such as SAC due to their finer micro-structure have been known to be susceptible to fracture under the influence of mechanical shock.

During in service conditions, thermo-mechanical fatigue cause failures due to CTE mismatches and thermal aging causes gradual coarsening both (phase and grain) that weakens the solder structure and makes it susceptible to failure in areas of high stress concentration. Authors also state that certain inter-facial reactions leading to brittle inter-metallic structures are accelerated as well. Humidity has also been mentioned as it leads to electro-migration and also causes corrosion.

2.2.2. Crack Initiation and Precipitation

While Eutectic alloys owing to their low melting point offer attractive medium for electronic manufacturing, they are also characterized by their inherently high homologous temperature, a factor, responsible for inducing creep strains in the solder joints [9]. Homologous temperature is defined as ratio of given temperature to melting temperature of alloy. Any value of homologous temperature that is greater than 0.5 is indicative of creep stress being predominant. For Pb37 solder the melting point is 456K, therefore at room temperature of 20°C which is 293K the homologous temperature of Pb37 solder is: 293K/456K = 0.642.

Creep strains in solder joints are temperature and time dependent stresses. As seen above, they are significantly predominant even at room temperatures or temperatures well below the specified operating temperatures for the product. For most applications where electronics is subjected to thermal stresses that are far above the room temperature the problem of creep becomes even more predominant and sets the stage for accelerated degradation.

Creep stresses induce strains in the solder joint that lead to stress relaxation over time causing the releasing of the energy in the system leading to irreversible deformation. This is marked by dislocation of slips planes. As established before exposure to elevated temperature promotes grain and phase coarsening that leads to fracture and crack precipitation. This occurs when the grain growth reaches the point when Slip planes can no longer glide along the lattice in direction of stress and are forced to climb up the lattice leading to permanent deformation.

The strains are induced due to mismatches in the CTEs that cause relative motion to occur between various elements bonded by solder.

Figure 17 below shows the creep mechanism. It is a function of applied stress and temperature. It is exhibited by two mechanisms namely, glide along the direction of stress and climb up when obstacle is encountered.

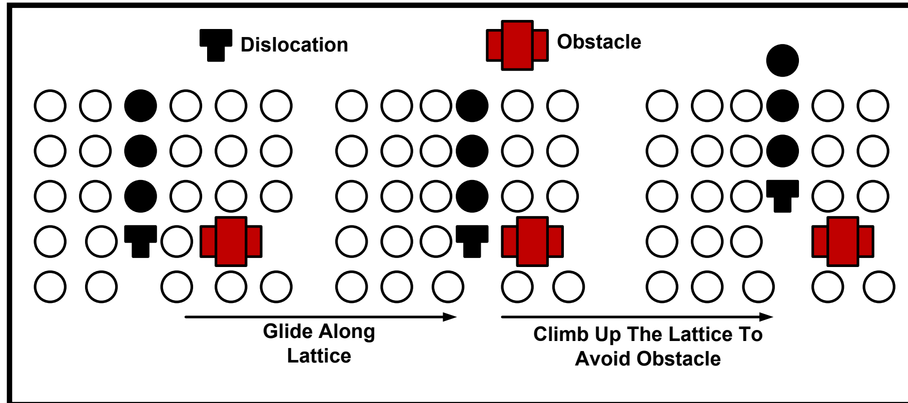

Figure 17. Glide and Climb Mechanism [9]

For thermal and power cycling, the strains rates of loading are of the order of 10^{-4}%/s, hence creep is dominant whereas for vibration the strain rates of loading are at least 10%/s hence creep is minimal [9].

Solder joints usually don't fail on exceeding the stresses acting on the solder joints beyond the strength limit during tests or in use [10]. However, they do fail over time under cyclic fatigue conditions by eventually succumbing to combination of constant and time varying strain loading that surpasses the fatigue limits. The author in the publication [10] has based his study only on through-hole (TH) component systems. Though the exact manifestations of failures encountered in [10] for TH components may differ from those in surface mount technology components (SMT- which are more prevalent these days) but basic underlying principles are still the same.

Author states that the strain conditions are generated due to differences in the coefficient of thermal expansions between various entities i.e. PCB and component lead/interconnect connected by means of a solder joint. One of the difficulties encountered in solder systems is in providing or implementing a strain relief mechanism that can mitigate creep strains that arise due to high homologous temperatures in such joints. The failure usually encompasses physical and metallurgical changes that occur in solder joints, nature of stress and stress modes in combination with temperature.

Author offers and insight into stress failure mechanism where presence of failure is described by dulling of the solder surface. This effect is due to displacements in PSBs occurring within the solder matrix comprising the joint. As solder is work hardened the grain growth between adjacent PSBs is impeded. The movement then occurs between other adjacent PSBs. This process continues until one band is that is weakened due to Pb-rich phase eventually fractures leading to stress relaxation due to which the load drops. Figure 18 reproduced from the publication explains the mechanism at work.

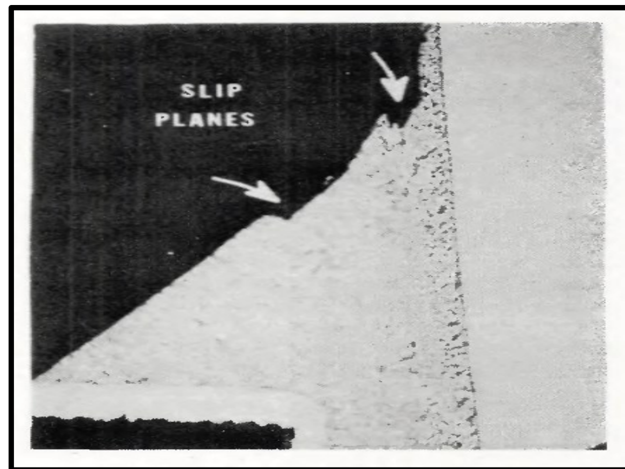

Figure 18. Slip Band Movements with Solder Matrix [10]

High stress low cycle failures will not have opportunity to undergo phase changes due to grain coarsening and hence it results into complete fracture of solder joint with no distortions on the surface. on the other hand low stress high cycle failures are marked by significant grain coarsening in high stress areas through which the fracture propagates.

Figure 19 and Figure 20, reproduced from the paper; show the differences in level of grain coarsening for high stress low cycle and for low stress high cycle failures. Grain coarsening is pretty evident in the latter case.

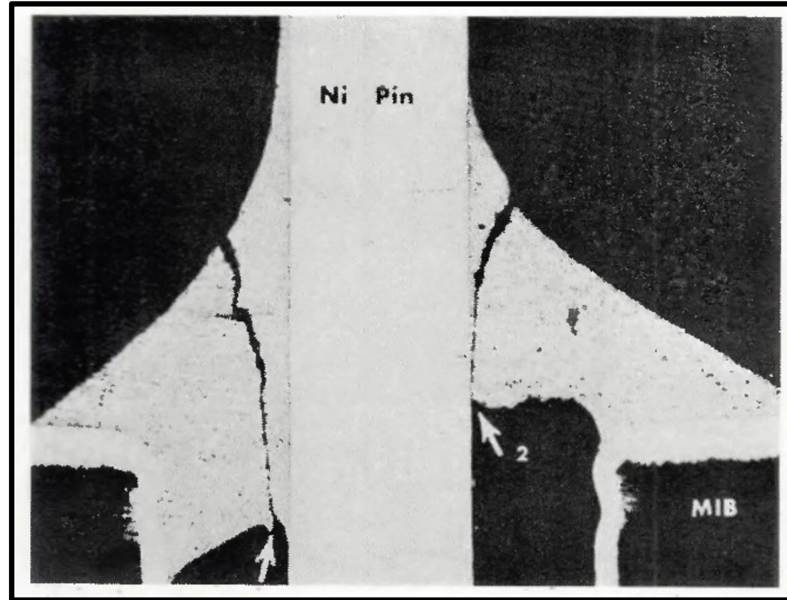

Figure 19. High Stress Low Cycle Failure [10]

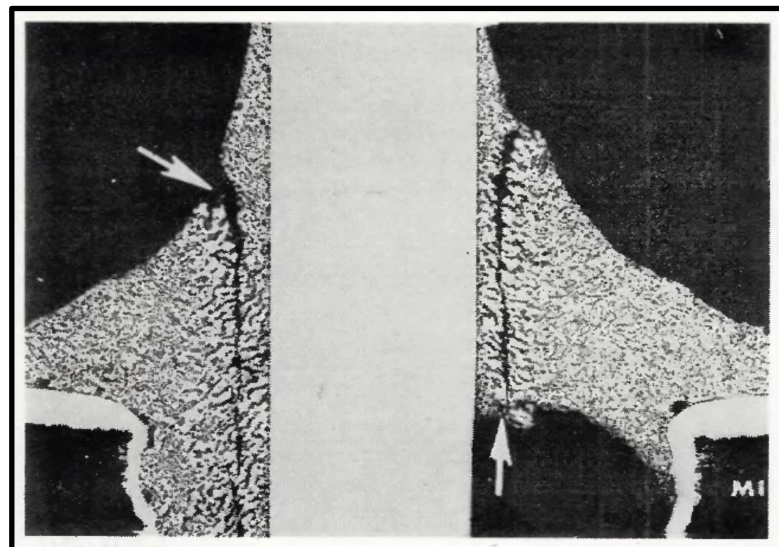

Figure 20. Low Stress High Cycle Failure [10]

Micro-structure evolution through deformation process that is concentrated in those areas that experience maximum shear strain in direction parallel to applied stress [17]. In Pb-Sn solders combination of stress and temperature results in stress assisted diffusion of material leading to Pb-rich phases. The grain growth associated with this phenomenon causes the grains to grow from sub-μm range to about 5-10 μm. Failure occurs when the grains can no longer slide or rotate causing impediment

to the slippage of PSBs. In Pb-Free solders phase coarsening takes place with minimal grain coarsening as these solders are 95% or more Sn.

Authors have also discussed the role of intermetallic compounds between pad metallization and active components of solder (mainly Sn). Authors state that even after solidification the intermetallic layers can grow through diffusion process to as much as 20 μm or more. This leads to voiding and also depletion of finish metal and loss of adhesion with inner base metal leading to separation. Structure of solder joint showing different phases is presented below in Figure 21.

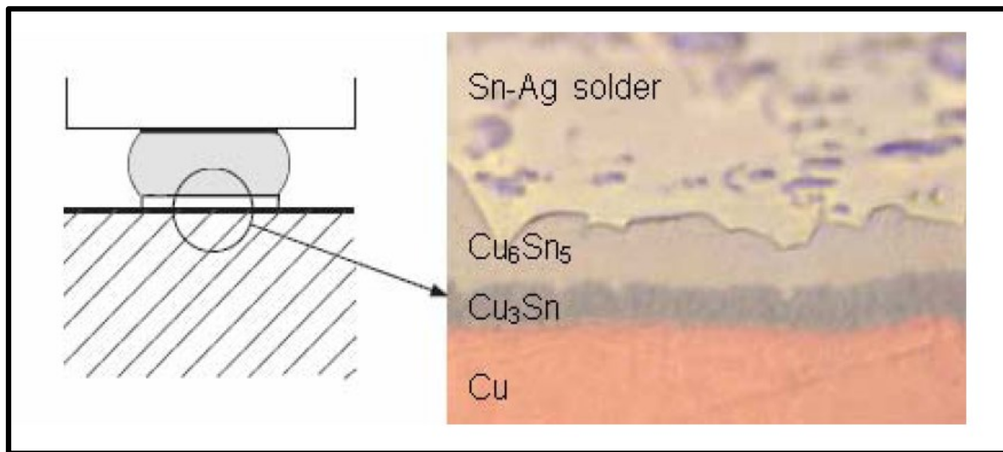

Figure 21. Pb-Free SAC Alloy Solder Joint of BGA Package [17]

The authors have also proposed the relationship below for intermetallic compound growth rate as a function of time and temperature:

$$x(t,T) = x_0 . A . t_n \exp^{\left(-\frac{Q}{RT}\right)} \tag{8}$$

where x is total intermetallic thickness, t is time in s, T is temperature in K, $\mathbf{x_0}$ is thickness of intermetallic as soldered, A and n are constants, R is universal gas constant and Q is the activation energy for intermetallic growth process.

2.3. Crack Propagation Phase in Failure of Solder Joints

Behavior of both Pb-Based and Pb-Free Solder joints have been extensively studied and cross-referenced in publication [5]. Solomon [5] has studied the behavior of Pb37 solder alloy in wide temperature ranges of -50°C, 35°C, 125°C and 150°C. His studies have proposed that modified Coffin-

Manson (CM) model was applicable with exponent $\alpha=0.5$ for temperature ranges of -35°C to 125°C and $\alpha=0.37$ at 150°C.

Author [5] has not dealt with grain coarsening mechanism but has pointed out to the fact that when the fractured solder joints are studied the ridges that mark the fracture have dimensions that are consistent with expected grain size due to grain coarsening phenomenon due to thermal energy transfer.

Author's [5] studies have utilized controlled strains to study plastic behavior of solder joints. Author points out that failed solder joints are direct result of fatigue which in turn is direct result of strain induced in the joint due to stresses induced by varying temperatures. The stresses are induced due to mismatches in CTE of various elements constituting the solder joint. The mismatch in CTE causes the joints to suffer strains due to stress concentration due to temperature gradients and thermal stresses.

Author points out the interactive nature of temperature and properties of solder joint. As the temperature changes so do the properties of solder joints (such as solder joint strength) hence it is very difficult to characterize the properties of solder joints under varying temperature conditions.

In the paper the author has adopted the approach of determining the fatigue behavior of solder joints at different temperature levels (of interest) where the different temperature levels cause different stress levels to achieve a given amount of plastic deformation and eventual failure.

Author has relied on Coffin-Manson model to explain the solder joint failure phenomenon mainly because of non-linear nature of plastic deformations. Since Coffin-Manson models are time independent models hence author has relied on modified Coffin-Manson model to incorporate cyclic and frequency effects. Coffin-Manson model used by author is given as:

$$\Delta\Upsilon_p . N_f^{\alpha} = \theta \tag{9}$$

where, α and θ are constants. $\Delta\Upsilon_p$ is the strain required to induce predetermined plastic deformation and N_f is number of cycles it takes to get to the failure point.

Author used the test specimens subjected to shear load in order to characterize the solder joint degradation. Load (stress) was applied through an automatic computer controlled set-up such that cyclic loads (both elongation and compression) at a predetermined strain level and rates were applied to the

solder joint under study. Failure point was specified where applied strain induced plastic deformation to the point that the Load (Stress) dropped to ½ of Initial Value at the corresponding temperature.

Author does further point out to limitations of Coffin-Manson and modified Coffin-Manson model due to couple of reasons. Firstly Coffin-Manson and modified Coffin-Manson models are power law models and therefore applicable only to non- linear deformations such as plastic deformations. Secondly some studies have used total strain data in Coffin-Manson model due to the involvement of elastic term. Inclusion of total strain however will lead to slope of Strain v/s Life plot to be less than ɑ value of Coffin-Manson expression determined by author.

Author argues that while elastic strain cannot be ignored in the solder joint system, the amount of elastic displacements within the solder joint are extremely small compared to large amount of non-solder elastic displacements in the system. Another argument author points to while relying on the works of R.N Wild [10] is that the cited study used strain values of more than 3% which according to author would lead to plastic strains to pre-dominate. Therefore, author resorted to subtracting the elastic component from the total strain expression as follows:

$$\Delta p = \Delta total_displacement - KP \tag{10}$$

where, P is applied stress.

HD Solomon [18] has presented the results of comparative study between Sn96, Pb40 and Pb96 eutectic alloys. The study primarily reinforces the fact that Sn96 shows superior fatigue resistance than Pb-Sn alloys. Like the author's previous work [5] involving only Pb40 solders this study also employed 2 copper test block specimens solder together for each type of solder and subjected them to shear stress loads. The applied strains in this case too were fully reversed limited plastic strain applied at a rate of about 0.3Hz. The study again relied on the premise as in case of (1) above that most metals follow Coffin-Manson law for low cycle fatigue. This is expressed by (9) above.

The experiment also employed an analog plastic strain computer to determine and compensate for system elasticity there by only accounting for plastic strains as shown in (10) above.

Though the author hasn't dealt with underlying mechanism of grain coarsening directly through energy transaction analysis however the methodology and observations of stress and strain data in the

experiments both in [5] and in the present case offer insight into the grain coarsening phenomenon. Figure 22 below is reproduced from paper [18]. It shows the hysteresis and load drop behavior which the author state is due to development and growth of fatigue cracks which author proposes could be used as a measure of crack growth.

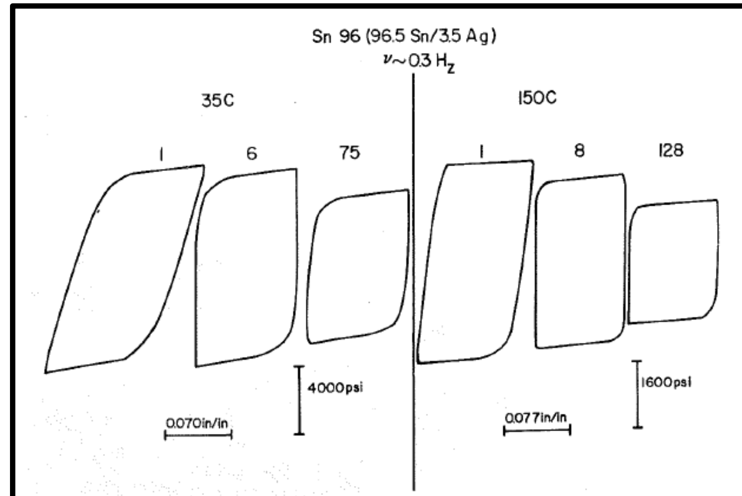

Figure 22. Hysteresis Loops Generated at 35°C and 150°C [18]

It can be seen from above figure that as the test progresses the area of hysteresis loop goes on decreasing due to decrease in the loading amplitude required for producing constant predetermined strain. Hysteresis is observed on account of completely reversed cycles in which an elongation cycle is followed by compression cycle.

The behavior of solder alloys under the influence of temperature and mechanical strains as described in the paper is consistent with well-established phenomenon of grain coarsening and which leads to formation of dislocation dipole between two adjacent slip planes.

Overall, the authors suggest for achieving maximum reliability the solder micro-structure should have the ability to resist formation of PSBs as these are the sites that lead to nucleation and eventual crack formation. One way achieve this is by homogenizing the deformation throughout the solder matrix thereby avoiding any localized stress concentration.

Creep is characterized by creep curve shown in the Figure 23 below [16]. It is defined by 3 distinct regions i.e. primary, secondary and tertiary creep. These are respectively denoted by decreasing strain rate, steady strain rate and increasing strain rate leading to material failure. Authors point out that

in most case for solder the strain rate is not extensive and is usually well characterized by steady state phase. Creep is thermally activated force and the constitutive equation for it is given as:

$$\dot{\gamma} = A\tau^{n}\exp^{-(\frac{Q}{KT})} \tag{11}$$

where $\dot{\gamma}$ is shear strain rate, τ is shear stress, n is stress exponent, Q is activation energy and T is temperature. Figure 23 below characterizes the creep for Sn-Pb solder and the values of n.

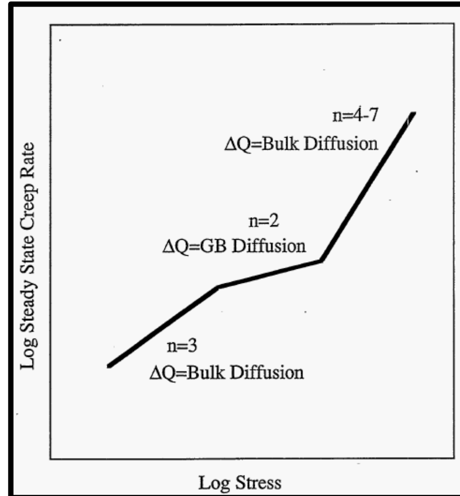

Figure 23. Sn Depletion Due to Intermetallic Layer Formation [16]

One of the direct results of creep is stress relaxation. The strains developed during processing or during thermal events in service create stresses in the solder joint. The stresses are then gradually relaxed by creep. The rate of stress relaxation is governed by steady state creep. The residual stress in joint under strain is given by:

$$\tau = G\gamma \tag{12}$$

where, G is shear modulus of elasticity and $\boldsymbol{\gamma}$ is shear strain. Stress relaxation under steady state condition is governed by rate equation which is obtained by differentiating (1) and substituting for $\dot{\boldsymbol{\gamma}}$ from (11) resulting in equation below:

$$d\tau / dt = GA\tau^{n}\exp^{-(\frac{Q}{KT})} \tag{13}$$

Fatigue is induced by cyclical thermal stresses and according to author since solder joints are characterized by high homologous temperature the cyclical thermal stresses cause fatigue that is largely induced due to creep.

Similar expressions for creep are defined in [9] and are given below:

I. Arrhenius equation for low stress range:

$$\varepsilon_c = A_o . \sigma^n . e^{(-Q/RT)} \tag{14}$$

where A_0, n are creep constants, Q is activation energy for dislocation motion, R is universal gas constant. ε_c is creep strain and σ is creep stress.

II. Garafalo equation for low to medium stress range:

$$\varepsilon_c = A_o[\sinh(\alpha.\sigma)]^n . e^{(-Q/RT)} \tag{15}$$

where, all the terms have same meaning as in (14).

III. Double power law equation to capture glide and climb dislocations:

$$\varepsilon_c = A_1(\sigma/E)^{n1} . e^{(-Q/RT)} + A_2(\sigma/E)^{n2} . e^{(-Q/RT)} \tag{16}$$

where, all the terms have same meaning as in (14).

Other publications have also dealt with nature of creep and its effects [17]. Relationship between creep, temperature corresponding strain induced in the solder joint is governed by following equation:

$$\Delta\gamma = \Delta\alpha . \Delta T . \frac{a}{h} \tag{17}$$

where, $\Delta\gamma$ is shear strain, $\Delta\alpha$ is the difference in the CTEs of joined materials, ΔT is temperature change, a is the distance from neutral point and h is the thickness of interconnect. Authors explain that the damage occurs due to natural tendency of solder joint to undergo stress relaxation which leads to movement and the change in the shape of joint. This change in the shape subsequently leads to areas of high stress concentration and coupled with other effects such as grain and phase coarsening leads to voiding or crack formation. Authors state that power law is usually used to describe the behavior of solders and is given as:

$$\dot{\epsilon} = A . \sigma_c^n \exp^{(-\frac{Q}{RT})} \tag{18}$$

where $\dot{\epsilon}$ is minimum strain rate, σ_c is critical flow stress, n is the stress exponent, Q is creep activation energy, R is universal gas constant and T is absolute temperature.

For solder joint reliability authors have proposed following variation of Coffin-Manson model.

$$N_f = \frac{1}{2}.(\frac{\Delta\gamma}{2\varepsilon_f})^{1/c} \tag{19}$$

where N_f is number of cycles to failure, $\Delta\gamma$ is total shear strain, ε_f and c are empirical constants.

Cohesive zone approach to model crack growth and to predict solder joint reliability by applying Weibull distributions to material failure has also been proposed [19].

Authors point out that one of the complexities involved in the solder joint reliability lies in the fact that there are is a large variety of components and packages that have different responses to same thermo-mechanical effects. More over properties of two popular solder mediums Pb-Based Pb-Sn (though being phased out due to RoHS initiatives is exempted from restrictions in Automotive) and Pb-Free SAC alloys are also different.

Authors state that traditional approaches to reliability estimation involve accelerated thermal cycling and then establishing Weibull parameters. Among the predictive model approaches various variations of modified Coffin-Manson models have been in vogue which are in mainly empirical modeling domain and do not address the basic Physics of Failure mechanisms at work.

Solder joint fatigue failure according to authors is fatigue crack growth problem and can be best explained by fracture mechanics framework. The relatively large scale size of fractures and plastic deformations do not allow use of linear elastic fracture mechanics frame work and associated laws like Paris-Erdogen Law.

The Cohesive Zone Model addresses the material behavior in the crack zone (process zone) which is different from material behavior in the bulk zone. Authors state that these behaviors can be built into FEA models if the direction of crack growth is known. But this approach presents challenges in terms of difficulty in establishing material parameters required for this approach. That is why empirical approaches tend to be more popular and widely used. Cohesive zone explains the fracture formation through separation of surfaces involving crack which is in turn resisted by cohesive traction.

One of the popular forms of traction separation used by authors is given as:

$$\mathrm{T} = \ \mathrm{e}.\sigma_c.\frac{\delta}{\delta_c}.\exp^{(-\frac{\delta}{\delta_c})} \tag{20}$$

where, σ_c is the maximum cohesive normal traction and $\boldsymbol{\delta_c}$ is characteristic opening displacement.

Authors quote Andres *et al* for definition of damage law used for cohesive model which is given as:

$$\mathrm{D} = \frac{\emptyset(\delta_c)}{G_C} \tag{21}$$

where, $\emptyset(\delta_c)$is area under traction separation curve from origin to instantaneous separation δ and G_C the critical energy for crack propagation.

Using above basis the authors have proposed hybrid model that resembles cohesive zone model developed from Weibull expressions. The probability density function (PDF) of a Weibull function is given as:

$$\mathrm{f(x)} = \begin{cases} \frac{\beta}{n^\beta}.\delta^{\beta-1}\exp^{(-\frac{\delta}{\beta})^\beta} & \text{for } x \geq 0 \\ 0 & \text{for } x \leq 0 \end{cases} \tag{22}$$

where, n and β are characteristic life and shape parameters respectively. Authors postulate that Weibull PDF may be used to describe point behavior of solder material undergoing fatigue and traction separation law can be written as:

$$\mathrm{T} = \frac{\beta}{n^\beta}.\delta^{\beta-1}\exp^{(-\frac{\delta}{\beta})^\beta} \tag{23}$$

Now cumulative distribution function (CDF) of Weibull distribution is given as:

$$\mathrm{F(x)} = 1 - \ \exp^{(-\frac{x}{n})^\beta} \tag{24}$$

Similarly, damage accumulation can be written as:

$$\mathrm{D} = 1 - \ \exp^{(-\frac{\delta}{\beta})^\beta} \tag{25}$$

In terms of inelastic strains this can be further written as:

$$\mathrm{D} = 1 - \ \exp^{(-\frac{\varepsilon}{\varepsilon_c})^\beta} \tag{26}$$

where, ε is total inelastic strain and ε_c is characteristic inelastic strain.

One term Taylor series expansion of above is given as:

$$\mathrm{D}_{n+1} = D_n + \frac{\partial \mathrm{D}}{\partial \mathrm{N}}\bigg| (\mathrm{N}_{n+1} - \mathrm{N}_n) \tag{27}$$

where, N_{n+1} and N_n are number of fatigue cycles at end of n+1 and n iterations. D_{n+1} and D_n are damage parameter at n+1 and n cycles. $\frac{\partial \mathrm{D}}{\partial \mathrm{N}}$ is established using finite differences. In order to establish the model parameters ε_c and β, authors carried out an experiment involving test samples and subjecting them to thermal cycling. They periodically observed the crack growth and established through dye and pry technique that crack growth resulted in reduction in the effective diameter of the joint at a rate that was constant at least in preliminary stage of crack growth. Thus, for every point two conditions for (26) were obtained for strains. One for damaged part at given number of cycles (correlated through constant rate condition) and other for reference as is condition. These two equations were substituted in (27) and solved simultaneously to get the parameters ε_c and β.

One of the primary basis for which the present study is being undertaken is to develop a comprehensive model for solder joint fatigue life. This study proposes to combine both the crack initiation phase and crack growth phase. Similar study by Liu *et al* [11] has been proposed to predict the "failure initiation time" and then perform reliability analysis using concept "reliability importance". The authors in [11] above-mentioned publication have proposed a combined model for process in which the degradation takes some time to manifest and the process is modeled as by following equation:

$$\mathrm{y_i(t)} = \mathrm{a_i} + \mathrm{e}^{(\mathrm{b_i}.\mathrm{t})} \tag{28}$$

where $\mathrm{a_i}$ and $\mathrm{b_i}$ are model parameters. The term $\mathrm{a_i}$represents degradation free zone and the term $\mathrm{e}^{(\frac{\mathrm{b_i}}{\mathrm{t}})}$ represents degradation at time t. Task of estimating the model parameters would be non-trivial if (28) was used as it is.

The degradation would have to be monitored continuously. Provided the measurement error in degradation is not significant. Once $\mathrm{a_i}$ and $\mathrm{b_i}$ are known the predicted initiation time can be estimated as shown below:

$$\mathrm{t_i} = \frac{1}{\mathrm{b_i}}.\ln(\frac{\mathrm{y_c}}{\mathrm{a_i}}) \tag{29}$$

Authors in [1] have attempted reliability analysis along with some FEA modelling. These aspects are discussed but not completely evaluated. Experimental work has been undertaken to evaluate 3 types for solder joints and results have been published in [1].

The paper mentions difference in the CTEs between the components, substrate (assuming PCB in this case) and solder joint as the reason behind induction of shear stresses leading to crack initiation and crack propagation leading to eventual catastrophic failure. The thesis extols the value and need for effort in the area of solder joint reliability due to huge dependence of today's products and services on electronics.

Reference is made to "homologous temperature cycling" (which is uniformly repetitive temperature cycling between two temperature limits and set ramp up/down rates) and "viscoplasticity" (which means rate dependent inelastic behavior of materials which are modeled or treated as continuous mass rather than discrete particles). It is mentioned that solder fatigue life is a complex phenomenon due to "viscoplastic" behavior of solder due to repetitive thermal cycling where temperature varies at certain predetermined rate, followed by dwell cycle and the cycles repeat at a certain rate.

While most of early work in the area of solder joint reliability involved extensive experimentation and analysis of results, increasing levels of miniaturization has led to changes in the way reliability assessment is approached these days.

I. A "constitutive model" is assumed out of variety of models available.
II. FEA model is developed using the constitutive equation and properties of materials involved. Predictive simulations are then carried out for various stress strain scenarios.
III. FEA results are then used to predict failure modes.
IV. This is followed by experimental verification of the FEA model.

Author has touched base on various approaches used for modelling solder joint fatigue. These are summarized below:

I. Plastic Strain Based Approach: Based on Coffin Mason Model plastic strain based approach is applicable for low cyclic fatigue. The stress concentration is high in this case to cause plastic deformation. In order to accommodate elastic strain situation modified CM models are used

that combine Basquin's model which accounts for elastic strain and therefore possibly crack initiation.

II. Time dependency: Since all reliability predictions are function of time) is added to modified CM model by adding the frequency term. So though modified CM model is used for reliability assessment, generally the CM model is not intended for elastic stresses and time dependent creep strain.

III. Creep Strain Based Approach: Creep strains are associated with long term exposure to mechanical stress (that can get induced due to factors such as temperature) while the stress are still under the yield strength. These are permanent distortions in shape due to grain boundary diffusion or matrix creep (dislocation movement).

IV. Energy Based Approach: Energy models are used to predict fatigue on the basis of Newtonian mechanics. Sum total of products of all the individual forces and their non-reversible displacements are numerically equivalent to non-recoverable work in a given cycle. This energy is considered as a measure of damage accumulation and is considered to dissipate across the entire interconnect. The energy based approach assumes the fracture will occur if energy accumulated in interconnect which dissipates most energy reaches a critical value.

V. Fracture Mechanics Based Approach: This approach assumes that a flaw or fracture or crack initiator always exists in any solder joint and it begins to grow under the stresses when subjected to mechanical stresses.

The effort of the study revolved around experimentation and study of three types of solder joints namely:

I. Barrel Shaped Solder Joints
II. Hour Glass Solder Joints
III. Double Barrel Stacked Solder Joints

Two sets 4 CSP packages each having 7 connection points were mounted on the board were used. These were thermally cycled and solder joint degradation was observed using Scanning Electron Microscope and Scanning Acoustic Microscopy.

2.4. Reliability Analysis

There is no dearth of material regarding reliability analysis in general. Various areas of electronics and solder joints have been widely covered under subject of reliability.

Liu *et al* [11] have dealt with subject of reliability involving initiation with degradation. This study undertakes the development of initiation with degradation time model to predict initiation and failure times. The two models are integrated taking into account conditionality of initiation phase incase degradation is initiated before give time at which reliability is being considered. A concept of reliability importance is introduced.

Yang *et al* [20] have put forward the treatment of reliability analysis involving damage accumulation approach. They have proposed the modelling strategy for damage accumulation where by damage accumulation is modeled as a function of time. This involves measuring variance of quality characteristic under consideration and modeling it through regression techniques. This model can then be used as time dependent variable as scale parameter for any location scale distributions for predicting damage accumulation at any given time. Rathore *et al* [21] have proposed the damage accumulation approach through linear transformation approach. Authors have used Palmgren-Miner's linear damage accumulation model and used an approach for one to one transformation for probability density function.

3. UNIFIED MODEL DEVELOPMENT

This chapter is devoted to building of the unified mathematical model that explains the solder joint behavior in crack initiation and crack propagation phases.

3.1. Model Background

Above background coupled with the insights from literature review sets the stage for the development of a unified thermo-mechanical model being considered for the present study. As is evident from expressions (5) and (6) above, the change in grain size can be a reasonable basis for ascertaining the length of crack initiation phase. However, being able to track the grain growth requires an expensive and elaborate measurement set-up and the whole process to undertake such a study is very time consuming. In a normal industrial setting this inference can still be made by monitoring the solder joint resistance and the change in resistance. Experimental set-up to monitor resistance can be accomplished quickly at a low cost providing a continuous set of measurements while the units under test are being monitored continuously, without the need for interrupting the data collection.

The key takeaway from foregoing passages also has been that the fatigue life can be defined as the number of cycles required or time it takes to reduce the load stress to a certain predetermined level of the original load (stress) required to induce a predetermined strain level. This reduction in load required to produce the same strain is due to reduction in the load bearing capacity of the solder joint due to coarsening nucleation which effectively reduces the load bearing cross sectional area due to formation of voids. While on one hand this leads to manifestation of a symptom i.e. measureable reduced load bearing capacity of solder joint, the same root cause also manifests in other measureable symptom i.e. increased electrical resistance of the solder joint.

Expression for electrical resistance is given as:

$$R = \rho . \frac{l}{A} \tag{30}$$

where, R is the resistance, ρ is specific resistance of given conductor material (here solder alloy), l is length of conductor and A is cross-sectional area of the conductor. We see from above (30) that as the

nucleation or grain growth progresses, reduction in net surface area of contact occurs and area A decreases. This leads to increase in R. Similarly, as the strains are induced due to thermo-mechanical events and mismatches due to CTE, given that volume of solder joint remains constant, they act to induce elongation and reduce the cross-sectional area and (deformation under stress) which also has a net result of increase in the resistance.

"Cubic coarsening model" has been proposed [8] as defined in (7) as a function of activation energy, temperature and applied strain. In line with the argument presented in the paragraph above we shall make necessary substitutions to correlate the parameters on the left hand side of (7) to reflect change in resistance. In doing so we obtain the expression below:

$$R(t_f) - R(t_0) = \frac{A.t}{T} \exp^{\left(-\frac{\Delta H_g}{RT}\right)} \left[1 + \left(\frac{\Delta T}{B}\right)^{n_c}\right] \quad (31)$$

where, A and B are new constants and rest of the terms are as defined in (7).

3.2. Model Data

For the purpose of modelling this study is reusing the data in [1] shown in the Figures 24 through 26 below:

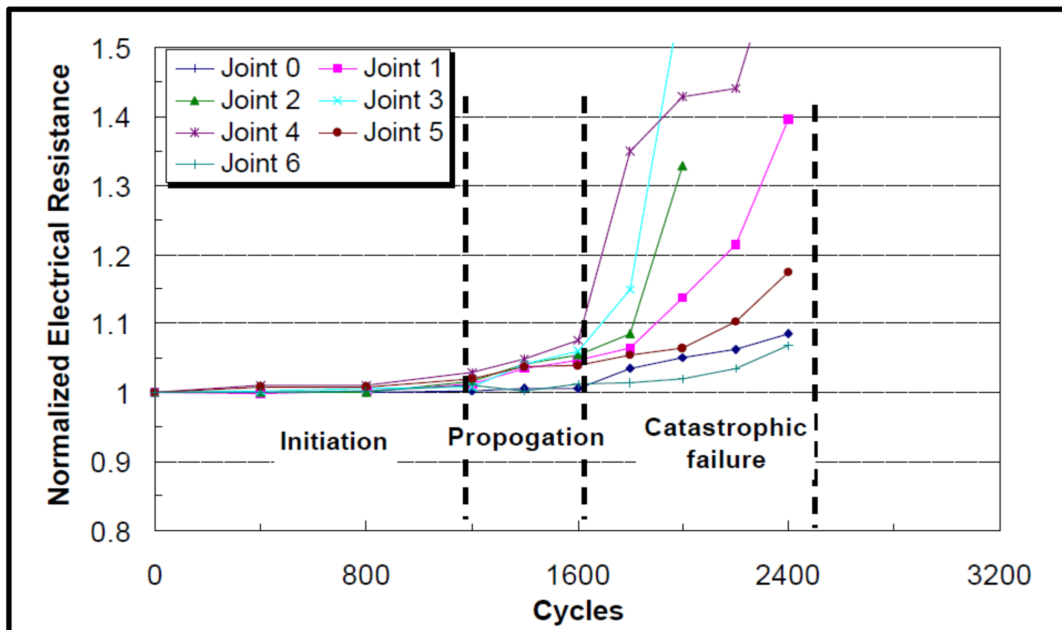

Figure 24. Configuration Single Barrel Configuration [1]

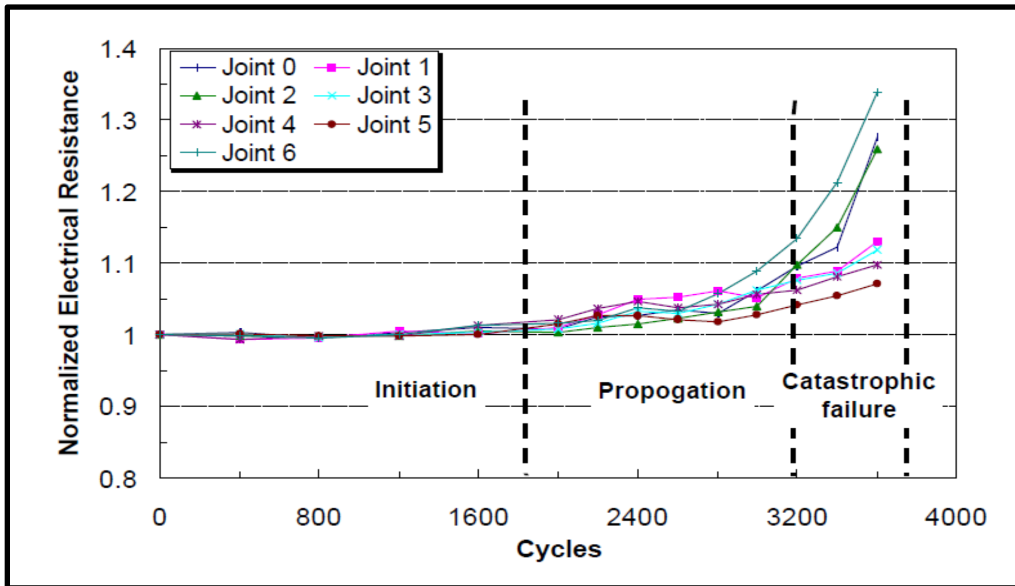

Figure 25. Configuration Hour Glass Barrel Configuration [1]

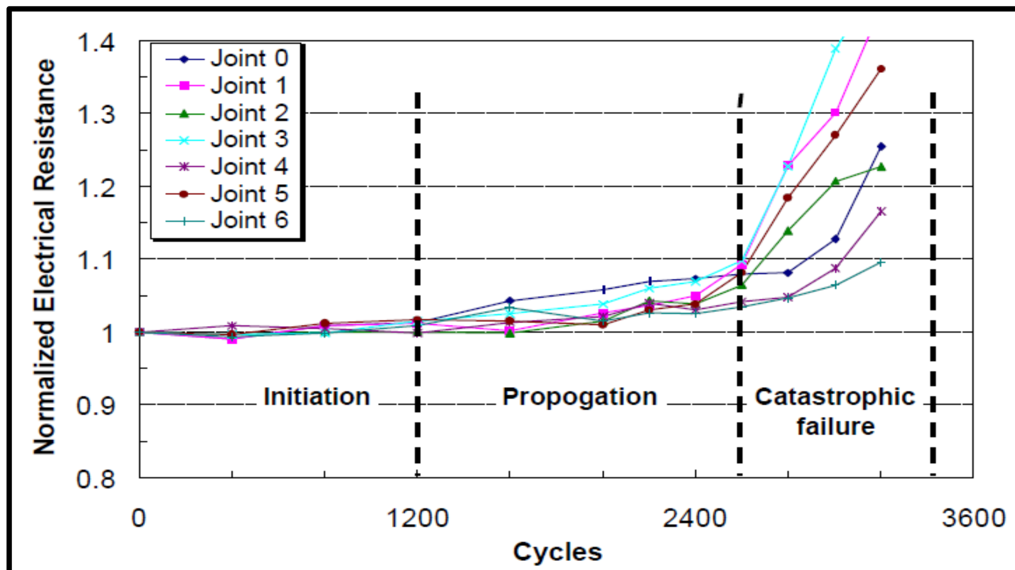

Figure 26. Configuration Double Barrel Stacked Configuration [1]

For each of the above cases, the study clearly depicts that the life cycle is divided into two distinct phases namely, crack initiation and crack propagation phases. Models in preceding works along the lines of this study [11] seek to combine the initiation and propagation phases together through a single empirical relationship as shown in (28). It is felt for purpose of this research undertaking that empirical relationships should not be used for crack propagation phase as exhaustive wealth of pre-

existing research is already in place that meticulously explains the behavior of solder joints in plastic domain. This research can be used in combination with a new initiation phase model to obtain an integrated unified thermo-mechanical model for solder joint fatigue life.

As far as the initiation phase goes it is the phase that leads to the genesis of crack. It may be noted that the crack is not initiated unless and until there is certain threshold of voiding that has been precipitated as is evident from Figure 12 We see in the aforementioned figure that the micro-cracks appear only after significant voiding has occurred. Another significant outcome of this observation is that though the void formation does not signify the crack precipitation it leads to reduction in contact surface area and therefore increase in overall resistance. This makes resistance measurement an attractive and simpler option as compared to other means. Moreover, it can be accomplished quickly, at low cost and enables continuous monitoring and measurement on units under test. A quick qualitative analysis shows that change in resistance can be as effective in evaluating degradation behavior both in crack initiation and crack propagation phases as shown in Figure 27.

3.3. Model Development

Figure 27 represents the change in resistance with respect to time or usage cycles. For model development, one of the initial things to do is to establish suitable threshold points, in terms of change in resistance value, to identify the end of crack initiation phase and crack propagation phases.

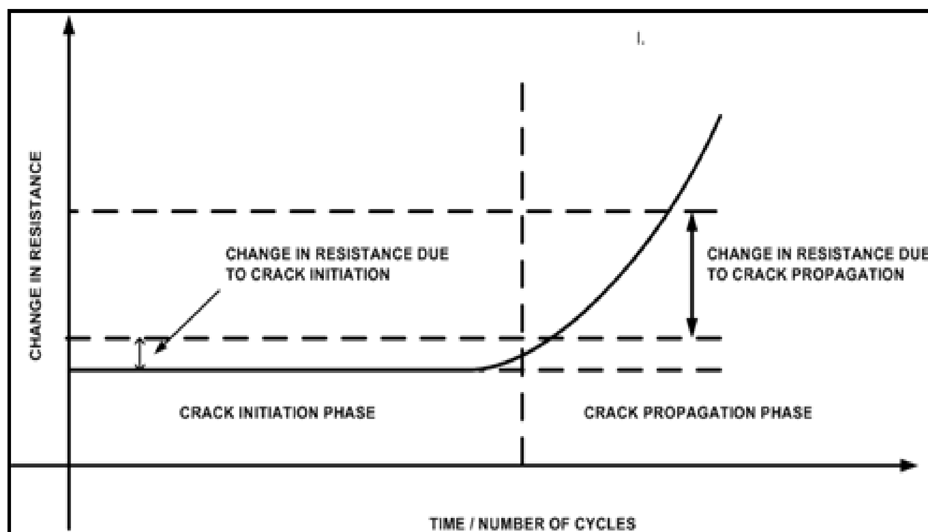

Figure 27. Change in Resistance during Crack Initiation Phase

Though solder joints have been a subject of great deal of research and publication, most of the research that has taken place and has been published has focused separately on two key phenomena i.e. grain coarsening (initiation phase) and degradation (growth phase). In order to devise a comprehensive model that encompasses both the above-mentioned phases it is imperative to first develop deeper understanding of individual phenomena and then devise methods to combine them together into a single unified comprehensive model.

3.3.1. Crack Initiation Phase Model Development

Cubic coarsening model has been proposed in [8] and is defined in equation (6) as a function of activation energy, temperature and applied strain. We see from equation (6), that as the nucleation or grain growth progresses, area of contact A, decreases due to voiding. This leads to increase in electrical resistance R. Similarly, as the strains are induced due to thermo-mechanical events and mismatches due to CTE, given that volume of solder joint remains constant, they act to induce elongation in length and reduction in cross-sectional area (deformation under stress). This also has a net result of increase in the electrical resistance. In line with the argument presented above modifying (6) by making necessary substitutions to correlate the parameters on the right hand side of (6) to reflect change in resistance we obtain following expression:

$$R(t_f) - R(t_0) = \frac{A.t}{T} \exp^{(-\frac{\Delta H_g}{RT})} \left[1 + \left(\frac{\Delta T}{B}\right)^{n_c}\right] \tag{32}$$

where, A and B are new constants and rest of the terms are as defined in (6).

Niu *et al* [11] have proposed degradation with initiation time phenomena through unified model given by expression below [11]:

$$y_i(t) = a_i + e^{(b_i.t)} \tag{33}$$

where, a_i and b_i are model parameters. The term a_i represents degradation free zone and the term $e^{(b_i.t)}$ represents degradation at time t. For given temperature range, material properties, and other operating conditions, other parameters except time in equation (32) will be unchanged and hence equation (32) can be reasoned as:

$$\Delta R(N_i) = \left[A + e^{(B.N_i)}\right] \tag{34}$$

where, A_0 and B_0 are new model parameters, which essentially capture the effect of operating conditions and other parameters, and N_i is number of cycles for crack initiation.

3.3.2. Crack Propagation Phase Model Development

Phenomenon of fatigue failure progression in solder joints has been widely researched and published mainly under the domain of Coffin-Manson and modified Coffin-Manson Models [1] [2] [4] [8] [11] [12] [13] [16]. There seems to be a wide spread consensus amongst the community of researchers that Coffin-Manson model explains the degradation/crack propagation behavior of solder joints really well. Coffin Manson model is basically a power law relation that correlates number of cycles to failure to applied strain as shown in (9). Modified Coffin-Manson Models have also been proposed [2] [5] [10] [18] [22] that introduce the cycling frequency as parameter and therefore provide correlation in terms of time to failure. Two such variations of modified Coffin-Manson models [5] [22] are shown below:

$$\left(N_f.f^{k-1}\right)^{\alpha}.\Delta\Upsilon_p = \theta \tag{35}$$

where, f is frequency, k is frequency scaling constant, α and & θ are constants and. $\Delta\Upsilon p$ is fatigue ductility parameter. Another modified form along the lines of Arrhenius equation is shown below:

$$N_f = C.f^m.(\Delta T)^{-n}.\exp^{\left(-\frac{Q}{R.T_{max}}\right)} \tag{36}$$

where, N_f is thermal fatigue life, C constant, f frequency, m is frequency scaling constant, ΔT is temperature range, n is temperature factor, Q is activation energy, R is Gas Constant and T_{max} is maximum temperature.

Coffin-Manson models in equations (9), (35) and (36) define fatigue life as the time it takes to reduce the load stress to a predetermined level of the original load (stress) required for inducing the same level of strain. This reduction in load required to produce the same strain is due to reduction in the load bearing capacity of the solder joint due to plastic deformation. While on one hand this leads to manifestation of a symptom i.e. measureable reduction in load bearing capacity of solder joint, the same root cause shall also manifest in other measureable symptom i.e. increased electrical resistance of the solder joint. Also strains due to mismatches in CTE will have the same bearing on resistance as discussed

in (30). Induced strains result in change in resistance of solder joints due to changes in shape parameters. Since the strain and length have proportional relationship and length and resistance have proportional relationship; we can substitute strain term in equation (9) with resistance. Therefore, modifying equation (9) and replacing ΔY_p with change in resistance $\Delta R_{i,f}$ we get:

$$\Delta R_{i,f} = D.N_p{}^d \tag{37}$$

where, D and d are model constants N_p is number of cycles from end of crack initiation phase to end of crack propagation phase.

3.3.3. Combined Model Development

Combining equations (34) and (37) we get the complete model that expresses change in resistance over initiation and propagation phases. This is expressed as:

$$\Delta R(N_{i,f}) = \begin{cases} A + e^{BN_i} & \text{Initiation Phase} \\ D.N_p{}^d & \text{Propagation Phase} \end{cases} \tag{38}$$

We see that both the terms in the expression (10) are nonlinear and hence methods for nonlinear regression can be suitably employed to deduce the model parameters.

Parameter of interest in any reliability study entails some measure of time and hence it is imperative that the proposed unified comprehensive model also should be expressed in terms of time. From (8) we get the initiation phase duration in terms of number of cycles for crack initiation to occur. This is given as:

$$N_i = \frac{1}{B}.Ln(\Delta R(N_i\ ) - A) \tag{39}$$

From (9) we get the propagation phase duration in terms of number of cycles given as:

$$N_p = \left(\frac{\Delta R_{i,f}}{D}\right)^{1/d} \tag{40}$$

Combining expressions (39) and (40), we get single unified expression that provides total duration to failure as a sum of number of cycles for initiation and propagation phases. This is given as:

$$N_f = N_i + N_p \tag{41}$$

3.4. Unified Model Parameter Estimation through Illustrative Example

To demonstrate the proposed modelling approach the experimental data given in Figures 24 through 26 derived from [1] was used. The aforementioned study used 3 sets of PCB mounted chip scale packages (CSP) with experimental parameters and operating conditions for the experiment as shown in Table 1 below:

Table 1. Set-up and Operating Conditions for the Experiment

Solder Bump Style	Sets	Joints	Stress Profile
Barrel Shaped Without Underfill	3	21	-40^{0}C to 125^{0}C, Ramp Rate 6.6^{0}C/min, Dwell Time 5 min
Triple Stacked Barrel Without Underfill	3	21	-40^{0}C to 125^{0}C, Ramp Rate 6.6^{0}C/min, Dwell Time 5 min
Hourglass/Column Shaped Without Underfill	3	21	-40^{0}C to 125^{0}C, Ramp Rate 6.6^{0}C/min, Dwell Time 5 min

In the original experimental study 3 solder bump styles were studied separately and 3 datasets were collected. However for the present study model the three data sets are combined together. This approach allows us to capture structural variability in account while estimating the model parameters. The plot of combined data set used in present study is shown Figure 28.

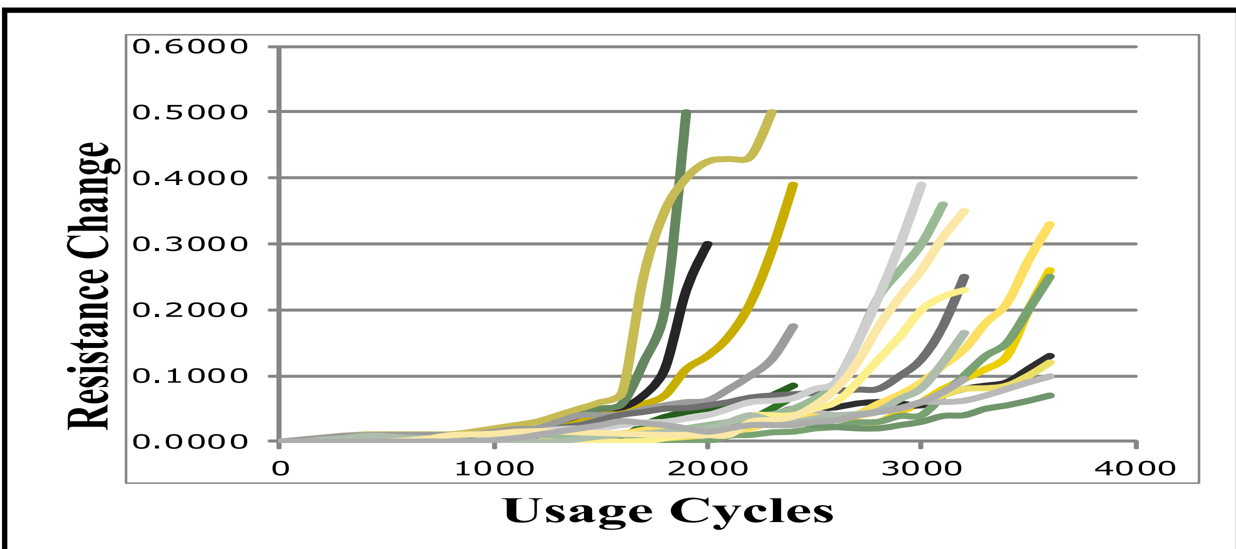

Figure 28. Combined Dataset for Model Parameter Estimation

3.4.1. Unified Model Parameter Calculation

The crack initiation phase threshold was kept at 3% change in the value of resistance. Whereas 10% change in resistance value is considered as threshold to mark the endpoint of crack propagation phase or solder joint failure. Non-linear regression techniques in MINITAB software were used to estimate the model parameters for both crack initiation and crack propagation phases using equations (34) and (37) respectively. Estimated parameter values for both the models are given in Table 2.

Table 2. Estimated Model Parameters

Phase	Parameter	Value	MSE
Crack Initiation	A_0	-0.00557	0.0000934
	B	$1.38508*10^{-5}$	
Crack Propagation	D	0.768758	0.0098343
	d	0.0473264	

3.4.1.1. Crack Initiation Model

Substituting the values of respective coefficients in equation (39) we have:

$$N_i = \frac{1}{1.38508 * 10^{-5}} . Ln(\Delta R(N_i) - (-0.00557)) \quad (42)$$

3.4.1.2. Degradation Model

Substituting the values of respective coefficients in equation (40) we have:

$$N_p = \left(\frac{\Delta R_{i,f}}{0.768758}\right)^{1/0.0473264} \quad (43)$$

3.4.2. Combined Model Mean Time to Fail Estimation

Using 3% and 10% change in resistance as threshold criteria equations (42) and (43) are used to estimate crack initiation and crack propagation durations respectively. The expected time for crack initiation, N_i is 2524 cycles and expected time for crack propagation N_p is 259 cycles. The total expected

life of solder joint, $N_f = N_i + N_p$ is 2783 cycles. We see from above estimates of lifetimes that the degradation phase is an order of magnitude shorter than initiation phase, which justifies our argument of modeling crack initiation phase separately. Further, as shown in Table 2 the error (difference between predicted and actual values) is not very high indicating good fit of the models for given the data set. It is considered good measure considering large variability in data as well as the model parameters which are dependent on operating conditions of experiment used to collect the data.

4. RELIABILITY ANALYSIS

Preceding analysis in chapter 3, dealt with the evolution of comprehensive unified model to predict expected mean life as a function of change in resistance of solder joint by modelling physics of failure/degradation behavior. However failure times of each individual units operating in field shall vary from one instance to another due to variability in operating conditions and inherent variability associated with each product. This inherent product variability arises due to many factors which can be termed as random variables such as types of solder joints, processing variations, solder joint material variability, PCB variability etc. Moreover process of determining the model parameters using regression techniques also introduces variability and hence model parameters also become random variables. Therefore, it is imperative to capture and analyze the extent of variability and establish the probabilistic measure of precision or certainty in the range of predicted quantities by the failure models.

Reliability analysis for the comprehensive model starts with determining suitable distribution models for both the phases namely, crack initiation time and failure time and the end of crack propagation phase. Figure 29 below represents the notion of crack initiation and failure time distributions for purpose of reliability analysis in the present study.

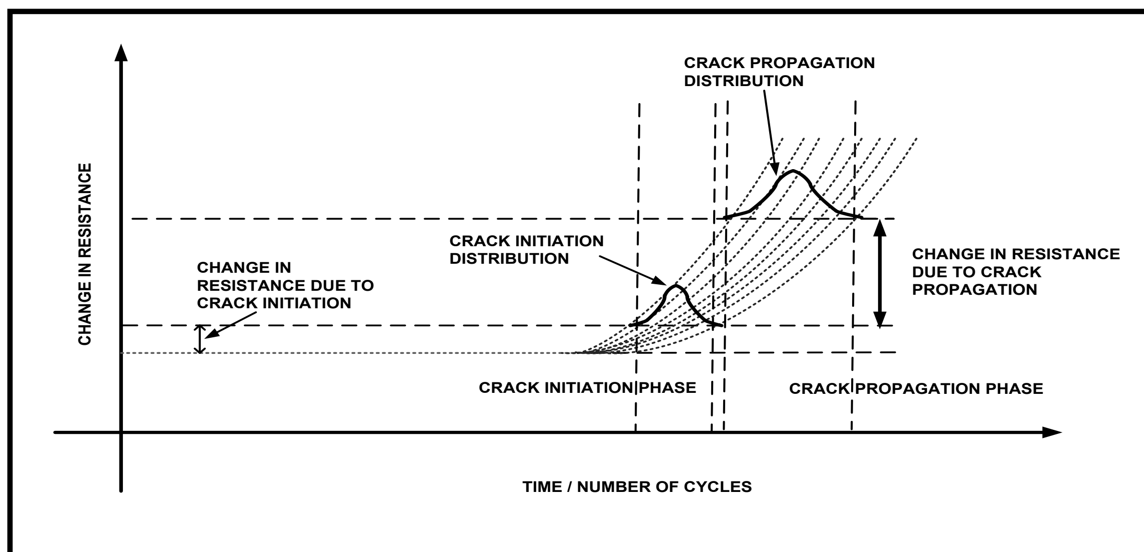

Figure 29. Distributions of Crack Initiation and Propagation Phases

The nature of two phases is marked by underlying physics of failure mechanisms at play that determine the type of distributions associated with the two phases.

The Initiation phase is predominantly marked with random phenomenon that has possibly the roots in process variations and other variations such as, operating conditions, [23] package styles of components, number of solder joints per package, PCB variations etc. These can all be argued to be random variables. The two distributions that distinctly capture the randomness are Normal and Exponential distributions. While Normal distributions are very general and can be applied to variety of situations, experience shows that exponential distributions have been widely used for applications such as electronic failures [23]. Therefore exponential distribution can be argued to be the distribution that defines the nature of the initiation phase. Not only does exponential distribution account for randomness in the initiation phase it also accounts for the non-linear behavior of this phase as well. Hence we consider using exponential distribution to capture the randomness in crack initiation time.

Failure time, on other hand is marked by degradation mechanisms that are not only non-linear in nature but also distinctintly mark the end phase of solder joint life and hence they embody the characteristics of that are clearly identifiable with crack propagation phase. The variability in this phase arises out of the variability due to initiation phases, variability of the operational conditions, variability in initial crack dimensions etc. The two distributions that deal with phenomena of non-linearity and wear out are Weibull and Log-normal distributions. As a matter of common experience it is known for most applications in electronics, log-normal distributions tend to be a better fit for failure data [20] and therefore we shall consider Log-normal distribution to capture probabilistic behavior of failure time to perform reliability analysis.

4.1. Reliability Models

The reliability analysis entails measuring failure rate of a given quality characteristic with respect to time (usage cycles). One method is to capture the probabilistic behavior failure time by determining the distribution around failure time. This is done by relying on experimentation by collecting and analyzing failure data to determine the best fit or relying on existing knowledge base regarding nature of

failure and failure time distributions. Second method is to evaluate reliability based on evaluating damage accumulation on the quality characteristic of interest. In this case time dependent dynamic models are needed to be evaluated.

4.1.1. Failure Time Distribution Approach

Failure time distribution approach shown in following sections considers applicable distributions at initiation and failure times to evaluate reliability of individual phases and then combines them to determine the total reliability.

4.1.1.1. Initiation Phase Reliability Model

The exponential model is initiation model chosen for reliability assessment of crack initiation model phase. Probability density function for exponential model in terms of distribution parameter(s) is defined as:

$$f(N_i;\lambda) = \begin{cases} \lambda.e^{\lambda.N_i} & Ni \geq 0 \\ 0 & N_i < 0 \end{cases} \tag{44}$$

where, N_i is no of cycles for initiation phase and λ is the distribution parameter also known as failure rate.

The expected life of for exponential distributions is given as:

$$\mu = \frac{1}{\lambda} \tag{45}$$

The variance of exponential distribution is given as:

$$\sigma^2 = \frac{1}{\lambda^2} \tag{46}$$

Cumulative distribution function for exponential distribution is given as:

$$F(N_i;\lambda) = \begin{cases} 1 - e^{\lambda.N_i} & Ni \geq 0 \\ 0 & N_i < 0 \end{cases} \tag{47}$$

Reliability function for exponential distribution is given as:

$$R(N_i) = (1 - F(N_i)) \tag{48}$$

Or:

$$R(N_i) = e^{-\lambda.N_i} \qquad \text{for } N_i > 0 \tag{49}$$

4.1.1.2. Propagation Phase Reliability Model

The log-normal model is chosen for reliability assessment of crack propagation phase. Probability density function for exponential model in terms of distribution parameter(s) is defined as:

$$f(N_p;\hat{\mu},\hat{\sigma}) = \frac{1}{N_p.\hat{\sigma}.\sqrt{2\pi}}\ e^{-\frac{(\ln N_p-\hat{\mu})^2}{2.\hat{\sigma}^2}}\ ;N_p \geq 0 \tag{50}$$

where, $\hat{\mu}$ and $\hat{\sigma}$ are location and scale parameters respectively. N_p is number of cycles for failure propagation.

Cumulative distribution function for log-normal distribution is given as:

$$F(N_p;\hat{\mu},\hat{\sigma}) = \frac{1}{2}\left[1 + \operatorname{erf}\left(\frac{(\ln N_p-\hat{\mu})}{\sqrt{2}.\hat{\sigma}^2}\right)\right]\ ;N_p \geq 0 \tag{51}$$

This, in simple form is also represented as:

$$F(N_p;\hat{\mu},\hat{\sigma}) = \Phi\left[\left(\frac{(\ln N_p-\hat{\mu})}{\hat{\sigma}}\right)\right]\ ;N_p \geq 0 \tag{52}$$

Reliability function for log-normal distribution is given as:

$$R(N_p) = \left(1 - F(N_p;\hat{\mu},\hat{\sigma})\right) \tag{53}$$

This in turn is given as:

$$R(N_p) = \left[1 - \Phi\left(\frac{\ln N_p-\hat{\mu}}{\hat{\sigma}}\right)\right] \tag{54}$$

4.1.2. Unified Reliability Model Considering Failure Time Approach

The equations (49) and (54) give the reliability of crack initiation and crack propagation phases respectively. Therefore in order to assess the total reliability both the reliability expressions have to be taken into account. However consideration of two different phases for reliability assessment is conditional in nature because of the variability in initiation time there is always some probability that for given cycle at time t, $N_t > 0$ degradation will set in. This is explained with help of Figure 30 below.

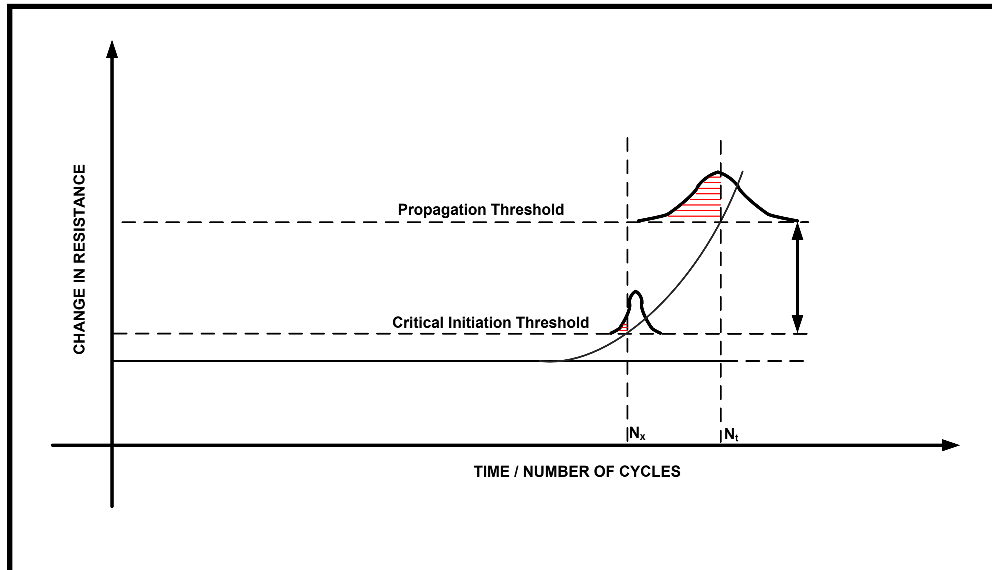

Figure 30. Conditionality of Degradation Phase Over Initiation Phase

As seen from Figure 30 above the conditionality arises from case where the degradation starts x cycles ahead of time t when we want to estimate the reliability as time t. This condition is similar to one explored by Liu *et al* [11]. The reliability in this case is given as:

$$R(N_t) = R_i(N_t) + R_p(N_t).\left(\int_0^{N_t} f_i(N_x;\lambda)dx\right) \tag{55}$$

Expression (55) can be written in terms of distribution parameters as:

$$R(N_t) = e^{-\lambda.N_t} + \left[1 - \Phi\left(\frac{\ln(N_t)-\hat{\mu}}{\hat{\sigma}}\right)\right].\left(\int_0^{N_t} \lambda.e^{\lambda.N_x}dx\right) \tag{56}$$

Above equation can be used to predict the reliability of solder joint model developed in this study at various cycles.

4.1.3. Reliability Modelling Considering Damage Accumulation Distribution Approach

Another approach is to determine and evaluate the probability distribution in terms of attribute that undergoes degradation or damage accumulation with respect to time or number of cycles as illustrated in Figure 31 below.

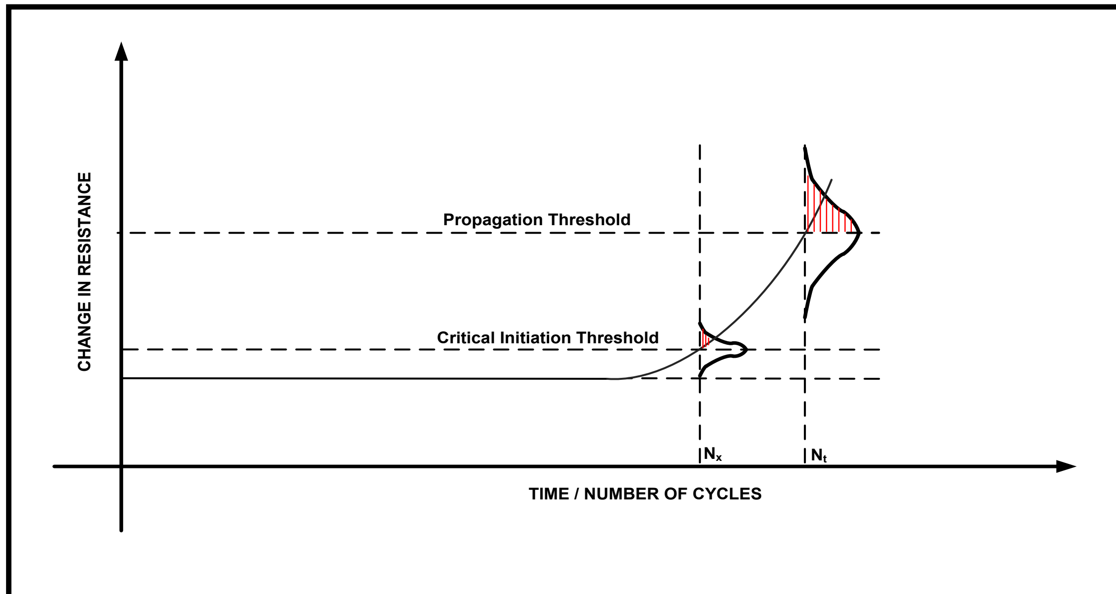

Figure 31. Change in Resistance Distribution

Yang *et al* [20] have demonstrated this approach which represents the variance in the measured resistances values at various instances in time. The resistance values at given number of cycles also exhibit random variation much like variation in failure times for a given resistance value threshold. These random variations can be explained using suitable distribution models such as normal distribution which can explain the random phenomena very effectively [20] . Therefore, for the purpose of this study we have assumed that resistance change exhibits a normal distribution $N(\mu_R(N_t), \sigma_R(N_t)^2)$, where, $\mu_R(N_t)$ is mean resistance at a given number of cycles N_t and $\sigma_R(N_t)^2$ is corresponding variance defining range of values about mean resistance $\mu_R(N_t)$ at N_t^{th} cycle.

As shown above, the location and scale parameters needed to model damage accumulation distribution are time (or usage cycle) dependent are hence they need to be modeled as dynamic or time dependent models. Modelling of location parameters has already been explained the in chapter 3 for both crack initiation and crack propagation phase. These models are expressed in equations (34) and (37). That leaves us with the scale parameter that is needed to determine degradation distribution.

As shown in Figure 31 , the variance in resistance value increases with time (usage cycles) as the solder joints undergo degradation to varying degree. This spread will increase over time as the degradation progresses.

This increasing trend in the shape parameter i.e. variance (or standard deviation) can also be modeled using least square regression techniques. Since variance increases monotonically, therefore it can be modeled as a linear function of number of cycles. [20] , as shown in the equation below:

$$\sigma_R(\mathrm{N_t}) = \mathrm{a} + \mathrm{b} * \mathrm{N_t} \tag{57}$$

where, a and b are regression coefficients that can be determined by fitting linear regression model to the test data.

Considering our earlier premise that resistance values are normally distributed, we can determine the reliability models in terms of resistance at the end of any given phase. Since the underlying distribution associated with the parameter change/degradation with respect to number of cycles is the same throughout the degradation period, a single expression used to assess reliability of both the phases. Normal failure probability density function is defined as:

$$\mathrm{f}(\mathrm{R_{Nt}}; \hat{\mu}, \hat{\sigma}) = \frac{1}{\hat{\sigma}.\sqrt{2\pi}}\, \mathrm{e}^{-\frac{(\mathrm{R_{Nt}}-\hat{\mu}_{\mathrm{Nt}})^2}{2.\hat{\sigma}_{\mathrm{Nt}}{}^2}}\ ; \mathrm{R_{Nt}} \geq \mathrm{R_0} \tag{58}$$

where, $\hat{\mu}$ and $\hat{\sigma}$ are location and scale parameters, R_{Nt} is the resistance at N_t^{th} cycle and R_0 is initial resistance. The cumulative failure density function is defined as:

$$\mathrm{F}(\mathrm{R}_{Nt}; \hat{\mu}, \hat{\sigma}) = \frac{1}{2}\, .\, \mathrm{erf}\left[\frac{(\mathrm{R}_{Nt} - \hat{\mu}_{Nt})^2}{2.\,\hat{\sigma}_{Nt}{}^2}\right]; \mathrm{R}_{Nt} \geq \mathrm{R_0} \tag{59}$$

This in simplified form is also expressed as:

$$\mathrm{F}(\mathrm{R}_{Nt}; \hat{\mu}, \hat{\sigma}) = \Phi\left[\frac{(\mathrm{R}_{Nt} - \hat{\mu}_{Nt})}{\hat{\sigma}_{Nt}{}^2}\right]; \mathrm{R}_{Nt} \geq \mathrm{R_0} \tag{60}$$

Reliability function for any phase is defined as:

$$\mathrm{R}(\mathrm{R}_{Nt}; \hat{\mu}, \hat{\sigma}) = 1 - \Phi\left[\frac{(\mathrm{R}_{Nt} - \hat{\mu}_{Nt})}{\hat{\sigma}_{Nt}{}^2}\right]; \mathrm{R}_{Nt} \geq \mathrm{R_0} \tag{61}$$

The expressions for total probability can be now be expressed by modifying equations (55) and (56) and rewriting them as:

$$\mathrm{R}(\mathrm{R}_{Nt}) = \mathrm{R}_i(\mathrm{R}_{Ni}) + \mathrm{R}_p(\mathrm{R}_{Nd}).\left(\int_0^{N_t} \mathrm{R}_i(\mathrm{R}_{Nxi}; \hat{\mu}_{Nx}, \hat{\sigma}^2{}_{Nx})\mathrm{dN}_x\right) \tag{62}$$

where, the first term $\mathrm{R}_i(\mathrm{R}_{Ni})$ on the right left above equation represents the reliability for the initiation phase. The second term represents the conditional probability for propagation phase when the resistance

value at given number of cycles exceeds the initiation threshold value due to degradation starting Nx cycles before Nt. Above expression can be written in terms of distribution parameters as:

$$R(R_{Nt}) = \left[1 - \Phi\left(\frac{R_{Ni} - \hat{\mu}_{Ni}}{\hat{\sigma}_{Nt}}\right)\right] + \left[1 - \Phi\left(\frac{(R_{Nt}) - \hat{\mu}_{Nt}}{\hat{\sigma}_{Nt}}\right)\right] . \left(\int_0^{R_{Nt_i}} \frac{1}{\hat{\sigma}_{Nx} . \sqrt{2\pi}} \ e^{-\frac{(R_{Nx_i} - \hat{\mu}_{Nx})^2}{2.\hat{\sigma}_{Nx}{}^2}} dR_{Nx}\right) \quad (63)$$

4.2. Reliability Modelling Example

To assess the reliability of solder joint we revisit the example discussed chapter 3 that was used to develop life prediction model. This section builds on the models developed in chapter 3 to formulate comprehensive reliability assessment models. Following sections provide the details of model formulation.

4.2.1. Failure Time Reliability Model Example

The exponential and log normal model distribution parameters for initiation phase and degradation phases are evaluated and given in Table 3 below:

Table 3. Rate and Location Parameters for Failure Time Reliability Modelling

Phase	Parameter	Symbol	Value	Remarks
Initiation	Mean time for crack initiation	1/λ	2257	Initiation phase mean time for exponential distribution
Propagation/Degradation	Mean time to Fail	μ	2516	Location parameter.
	Standard Deviation	σ_x	0.09	Scale parameter for log-normal distribution
	Ln(Mean time to Fail)	μ_{lnx}	7.83043	Location parameter for log-normal distribution

Substituting these parameters values in equation (56) we get failure time based reliability model as given in equation below:

$$R(N_t) = e^{-\frac{1}{2257}.N_t} + \left[1 - \Phi\left(\frac{\ln(N_t) - 7.83043}{0.09}\right)\right] . \left(\int_0^{N_t} \frac{1}{2257} . e^{-\frac{1}{2257}.N_x} dNx\right) \quad (64)$$

4.2.2. Damage Accumulation Reliability Model Example

For considering probabilistic damage accumulation model time dependent (usage cycles) models for mean and standard are the foremost requirement. The models represented in equations (34) and (37) provide the dynamic mean values for initiation and degradation phases respectively. The dynamic model for standard deviation is calculated by fitting least square regression to dataset in reference [1]. Thus we have the dynamic models for both the mean and standard deviation. The resistance thresholds for initiation and degradation phases are used as threshold values for determining reliability of each phase. Table 4 below provides the model parameters estimated from data.

Table 4. Location and Scale Parameters for Damage Accumulation Reliability Modelling

Phase	Parameter	Symbol	Value	Remarks
Initiation	Initiation phase resistance threshold	R_{Ni}	1.03	
	Initiation Phase Model Coefficients	A0	-0.00557	
		B	$1.38508*10^{-5}$	
Propagation/ Degradation	Mean time to Fail	R_{Nd}	1.1	
	Degradation Phase Coefficients	D	0.768758	
		d	0.0473264	
	Std. Dev	A	-0.004963	Intercept
		B	0.000028	Slope

The regression model for dynamic standard deviation is given in equation 65 below:

$$\widehat{\sigma_{Nt}} = -0.004963 + 0.000028 * N_t \tag{65}$$

Substituting parameter values from Table 4 in equation (64) we get damage accumulation reliability model for the data used in present study reference [1] given in equation below:

$$R(R_{Nt}) = \left[1 - \Phi\left(\frac{\hat{\mu}_{Ni} - 1.03}{\hat{\sigma}_{Nt}}\right)\right] + \left[1 - \Phi\left(\frac{\hat{\mu}_{Nt} - 1.1}{\hat{\sigma}_{Nt}}\right)\right] \cdot \left(\int_0^{1.1} \frac{1}{\hat{\sigma}_{Nx} \cdot \sqrt{2\pi}} \, e^{-\frac{(\hat{\mu}_{Nt} - 1.1)^2}{2 \cdot \hat{\sigma}_{Nx}^2}} dR_{Nx}\right) \tag{66}$$

Total reliability trends were calculated for both the failure time and damage accumulation models and the results are presented in in following sections.

Figure 32 below shows failure time distribution reliability trend.

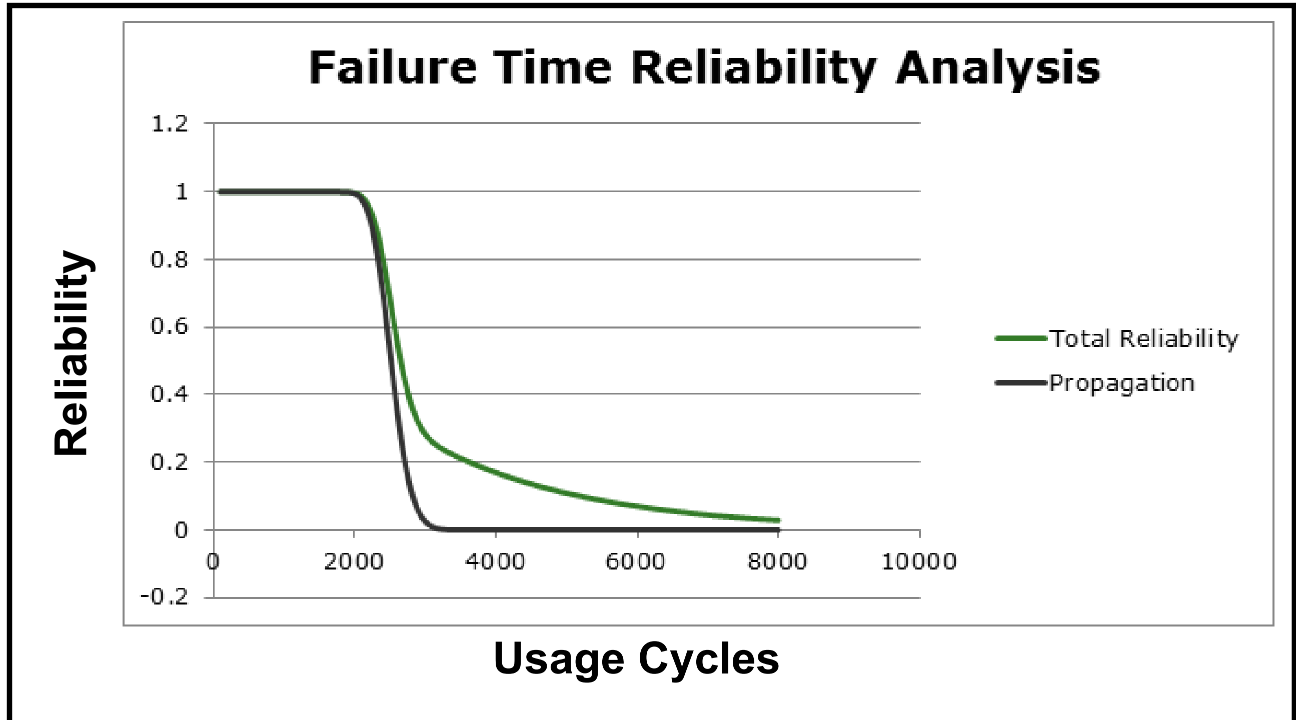

Figure 32. Failure Time Reliability Trend

Figure 32 above shows the comparison between total reliability and degradation model reliability for failure time distribution. We see from above figure that just accounting for degradation reliability tends to underestimate the overall reliability. Also we notice that overall meantime to failure as predicted by our model in equation (38) is in agreement with the mean time (at 50% reliability) as predicted by total reliability trend line.

Figure 33 shows the comparison between total reliability and degradation model reliability for damage accumulation distribution. As seen in Figure 32 we see the consistency in the trends for total reliability v/s degradation reliability.

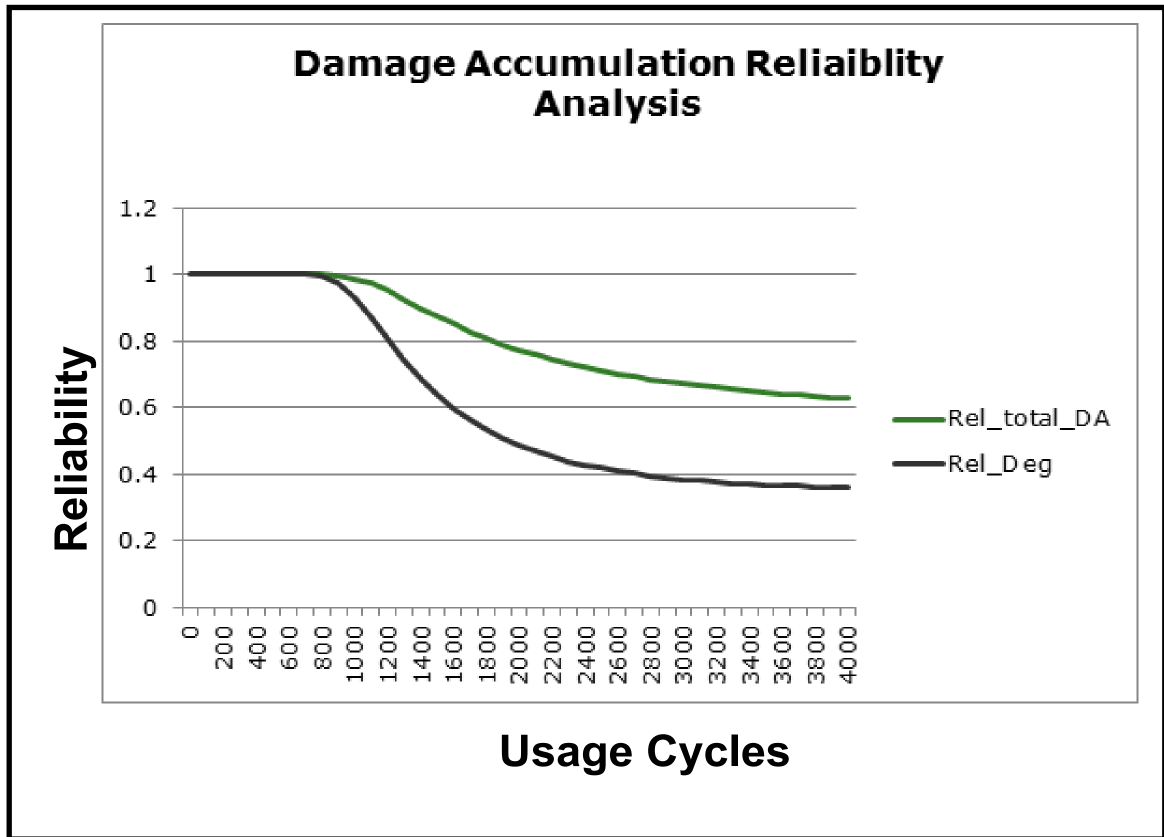

Figure 33. Damage Accumulation Reliability Trend

Thus, the two figures above validate the premise that not accounting for initiation phase in reliability modelling underestimates the overall useful life for the solder joints. Other implication which the above reliability analysis has is insight into reliability importance for each phase. This can help drive targeted reliability improvement focused delivering maximum returns.

5. SUMMARY AND CONCLUSIONS

The proposed study has developed and proposed a unified physics of failure based thermo-mechanical model for solder joint degradation and its reliability analysis. Motivation for undertaking this research study is multifold. Solder is a fundamental medium of choice for bonding components to PCB and for providing a good electrical and mechanical support in the process. The eutectic nature and inherently high surface energy characteristics of solder material that is essential for good wetting properties in turn makes the solder susceptible to degradation mechanisms right from the point of being *as manufactured*. All this makes solder and solder joints perfect candidates for study since the reliability of solder joint becomes fundamental factor that contributes to the product reliability. Above all, there aren't many studies that have dealt with solder joint degradation behavior in an integrated manner.

The proposed study captures the behavior of solder joints under the influence of thermo-mechanical stresses in a comprehensive manner. Basis for this approach lies in the fact that degradation phenomena are usually preceded by an initiation phase during which the time thermo-mechanical stresses cause the solder joints to undergo grain/phase coarsening leading to voiding and eventual crack precipitation. The unified model development part of this study deals with physics of failure mechanism and uses the data in reference [1] to develop a unified model that completely explains the initiation and degradation phases of solder joint life.

Dataset from study mentioned in reference [1] has been used to establish graphical and mathematical criteria for life prediction model development for crack initiation and degradation phase separately. This study combines and uses the total data set for all types of solder joints in above reference. Doing so allows us to capture the structural variability in the solder joint model. Change in resistance as a measure of degradation in quality characteristic has been used. 3% change and 10% change have been used as threshold criteria for initiation and degradation phases respectively. Nonlinear regression techniques using MINITAB software have been used to develop the individual models for each phase which are then combined to come up with a unified comprehensive model. Low value for mean square error points to validity of individual models that constitute the comprehensive unified model.

The model has been used to predict the mean life individually for initiation, degradation phases and to predict mean time to failure. The results from this study validate the premise of modelling initiation and degradation times separately. The study shows that for given data and operating conditions the initiation phase outlasts the degradation phase by almost an order of magnitude. This gives us a deeper insight into the behavior of two phases and to establish the grounds for any targeted reliability improvement efforts.

Establishing the comprehensive model is a prelude to performing reliability analysis on the model. The model can only predict the mean time to end point for each phase and for the total life. It does not provide any probabilistic range of certainty around the mean value. Therefore, in order to perform the reliability assessment, probabilistic distributions were taken into account based on the physics of failure mechanisms that define the failure distribution profiles for each phase. The reliability analysis took into account the individual phases to establish the conditional relationship for the unified reliability model. Since the degradation is preceded by initiation phase hence the variability in expected values may cause degradation to either set in much before or much later as defined by distributions for given phase. Therefore, while evaluating total reliability the initiation phase reliability for each time (usage step) is added with conditional reliability of degradation phase which is product of probability of degradation in initiation phase and reliability of degradation phase.

Reliability analysis was performed by taking into account both the failure time distribution approach and damage accumulation approach. The failure time approach reliability was evaluated by considering exponential distribution for meantime in the initiation phase. Exponential distribution typifies the randomness that is associated with the initiation phase and hence appropriately defines this phase. Log-normal distribution was used for degradation phase which is associated with wear out behavior, as both Log-normal and Weibull distributions describe the wear out phenomena appropriately.

For damage accumulation approach normal distribution was taken into account as the damage distribution can be very well envisioned to be a random phenomenon. Hence the normal distribution is appropriate choice for describing the damage accumulation. The target degradation thresholds of 3% and 10% change in resistance were taken into account for initiation phase and degradation phase reliability

components respectively. Normal distribution in this case needed mean and standard deviation as function of time (usage cycle) as distribution parameters. While mean value was easily established using the comprehensive model, standard deviation was evaluated by least squares regression fitting on the data set used for this study [1].

Reliability trends for both the failure time and damage accumulation models was calculated as summarized in Table 5 and shown in Figure 34. Looking at the values predicted by the failure time reliability model we find that time corresponding to 50% reliability from Figure 35 is roughly 2700 cycles which is close agreement with the mean time to failure predicted by the life prediction model. This not only points to validity of model but also validates the choice of distributions considered for failure time reliability modelling.

As is the case with any research undertaking, the present work culminates with insight, ideas and groundwork for future improvements and further research. With regards to future work the present models can be enhanced by incorporating into them the variables and terms to account for various operating conditions and parameters. This will allow the life time prediction based on other parameters by allowing users to vary various stress levels and evaluate their effects on individual phases and overall life of the product. Comprehensive DOE and ANOVA efforts can then be under taken to optimize the design parameters based on operating conditions to maximize the warranty period and design life time of products. Similar approach has been proposed by Yang *et al* [20] where they have incorporated elements of Taguchi's robust design methodology for reliability improvement. Use of joint probability distributions could be explored to evaluate combined failure time reliability with damage accumulation to a better insight into reliability behavior.

BIBLIOGRAPHY

[1] X. Liu, "Processing and Reliability Assessment of Solder Joint Interconnection for Power Chips," PhD Thesis, Feb 2001.

[2] W. Engelmaier, "Solder Joints In Electronics: Design For Reliability".

[3] C. Rauta, A. Dasgupta and D. C. Hillman, "Solder Phase Coarsening, Fundamentals, Preparation, Measurement and Prediction".

[4] A. Rollett, "Grain Boundary Surface Energy Measurement - Lecture 22," 2006. [Online].

[5] H. D. Solomon, "Fatigue of 60/40 Solder", IEEE Transactions On Components, Hybrids And Manufacturing Technology, Vols. VOL. CHMT-9, NO. 4, Dec 1986.

[6] Callister, Material Science and Engineering: An Introduction 7th Edition, Ch9. Fig 9.8., New York, New York: John Wiley and Sons, 2000.

[7] B. S. H. Royce, "https://www.princeton.edu/~maelabs/mae324/glos324/dislocationdipole.htm," Nov 2001. [Online].

[8] A. Dasgupta, P. Sharma and K. Upadhyayula, "Micro-Mechanics of Fatigue Damage in Pb-Sn Solder Due to Vibration and Thermal Cycling," InternationalJournalof DAMAGE MECHANICS, vol. 10, April 2001.

[9] A. E. Perkins and S. K. Sitaraman, Solder Joint Reliability Prediction for Multiple Environments, Spriinger.

[10] R. Wild, "Fatigue Properties of Solder Joints," Welding Journal (Welding Research Council), 1972.

[11] H. Guo, A. Gerokostopoulos, H. Liao and P. Niu, "Modeling and Analysis for Degradation with an Initiation Time," IEEE, Vols. 978-1-4673-4711-2/13, 2013.

[12] D. Dye, "MSE104 Microstructure and Properties of Materials," Imperial College London, [Online]. Available: http://dyedavid.com/mse104/.

[13] J. S. Hwang, H-Technologies Group, SMT Online Magzine, November 2012.

[14] A. F. Bowler, "Applied Mechanics of Solids," [Online]. Available: http://solidmechanics.org/Text/Cpter3_7/Chapter3_7.php.

[15] B. Cemal and J. Jianbin, "Measuring intrinsic elastic modulus of Pb/Sn solder alloys," Mechanics of Materials , vol. 34 (2002) 349–362, 2002.

[16] M. J. J.W. and R. H.L, "The Influence of Microstructure on the Mechanical Properties of Solder," in Society for Experimental Mechanics., Nashville, TN, June - 1996.

[17] L. Emil, H. Erika, S. Beáta, K. Ingrid and U. Koloman, "Solder Joint Reliability".

[18] S. Harvey, "Low Cysle Fatigue of Sn96 Solder with reference to Eutectic and High Pb Solders".

[19] D. Bhate, D. Chan, G. Subbarayan and L. Nguyen, "Fatigue Crack Growth and Life Descriptions of Sn3.8AgO.7Cu Solder Joints:A Computational and Experimental Study," in Electronic Components and Technology Conference, 2007.

[20] Y. Kai and Y. Guangbin, "Robust Reliability Design Unsig Environmental Stress Testing," Quality and Reliability Engineering, 1998.

[21] R. Vijay, O. Yadav, A. Rathore and R. Jain, "Probablistic Modelling of Fatigue Damage Accumulation for Reliability Prediction," International Journal of Quality, Statistics and Reliability, 2011.

[22] S. Ikuo, M. Hideo and Y. Ori, "Solder Joint Reliability of Chip Scale Packages using Modified Coffin Manson Model," Microelectronics Reliability, vol. 44, pp. 269-274, 2004.

[23] "MIL-HDBK-217F".